Maxim Yu. Khlopov

Virtual Institute of Astroparticle physics, Paris, France;
National Research Nuclear University “MEPHI”
(Moscow Engineering and Physics Institute) Moscow, Russia
and
Institute of Physics, Southern Federal University, Rostov on Don, Russia

Recent advances of Beyond the Standard Model cosmology

Talk at XXVI Bled Workshop "What comes Beyond the Standard Models?"

Bled, Slovenia 16 July 2023

Outlines

- BSM Physical basis of the SM cosmology
- BSM cosmology that follows from BSM physics.
- Primordial Black Holes (PBHs) as cosmological reflection of particle symmetry.
- Strong Primordial nonhomogeneities and Massive PBH clusters from models of inflation.
- Antimatter as profound signature for nonhomogeneous baryosynthesis.

Composition of the Modern Unverse

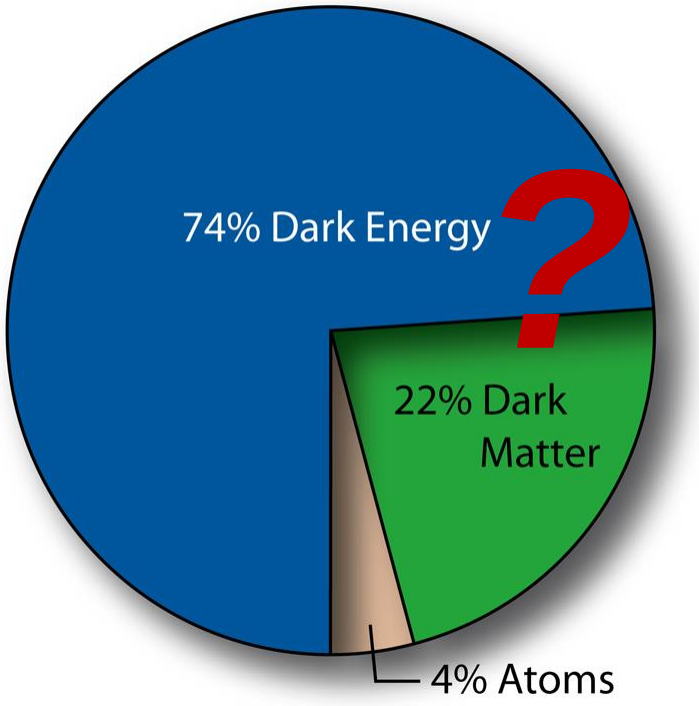

$$\Omega \equiv \frac{\rho}{\rho_{cr}}$$

$$\Omega_b \approx 0.044 \qquad \Omega_{CMB} \approx 0.5 \cdot 10^{-4}$$

$$\Omega_{DM} \approx 0.20$$

$$\Omega_\Lambda \approx 0.7$$

$$\Omega_{tot} \approx 1.0$$

In the modern Universe dominate dark energy and dark matter – their nature is related to the new physics – physics beyond the Standard model, on which the bedrocks of modern cosmology are based

The bedrocks of modern cosmology

Our current understanding of structure and evolution of the Universe implies three necessary elements of Big Bang cosmology that can not find physical grounds in the standard model of electroweak and strong interactions. They are:

- Inflation
- Baryosynthesis
- Dark matter/energy

Physics beyond the Standard model, describing these phenomena inevitably predicts additional model dependent effects, in which NS and BH play important role.

Cosmological Reflections of Microworld Structure

- **(Meta-)stability of new particles reflects some Conservation Law, which prohibits their rapid decay. Following Noether's theorem this Conservation Law should correspond to a (nearly) strict symmetry of microworld. Indeed, all the particles - candidates for DM reflect the extension of particle symmetry beyond the Standard Model.**
- **In the early Universe at high temperature particle symmetry was restored. Transition to phase of broken symmetry in the course of expansion is the source of topological defects (monopoles, strings, walls…).**
- **Structures, arising from dominance of superheavy metastable particles and phase transitions in early Universe, can give rise to Black Holes, retaining in the Universe after these structures decay.**

Cosmological Dark Matter

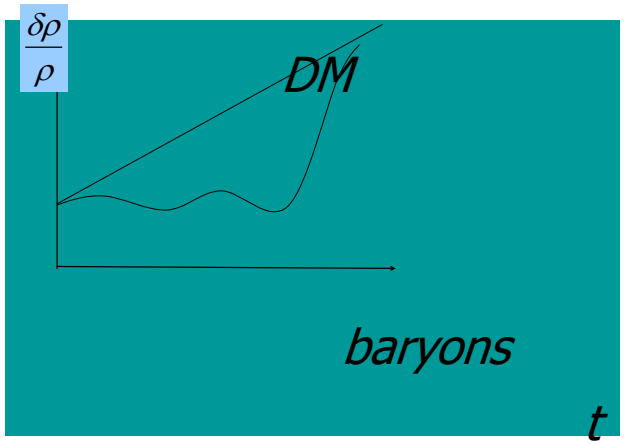

$$\frac{\delta\rho}{\rho} \Rightarrow \frac{\delta T}{T}$$

Cosmological Dark Matter explains:

- ***virial paradox in galaxy clusters,***
- ***rotation curves of galaxies***
- ***dark halos of galaxies***
- ***effects of macro-lensing***

But first of all it provides formation of galaxies from small density fluctuations, corresponding to the observed fluctuations of CMB

To fulfil these duties Dark Matter should interact sufficiently weakly with baryonic matter and radiation and it should be sufficiently stable on cosmological timescale.
Baryon density estimated from the results of BBN (mainly from Primordial deuterium) is not sufficient to explain the matter content of the modern Universe

Dark Matter – Cosmological Reflection of Microworld Structure

Dark Matter should be present in the modern Universe, and thus is stable on cosmological scale.

This stabilty reflects some Conservation Law, which prohibits DM decay.

Following Noether's theorem this conservation law should correspond to a (nearly) strict symmetry of microworld.

BSM physics of dark matter

- Extension of SM symmetry provides new conservation laws and stability of lightest particles that possess new conserved charges (R-parity in Supersymmetry, mirrority of mirror (shadow) matter, PQ symmetry in axion models etc)
- Mechanisms of symmetry breaking in the early Universe lead to primordial nonlinear structures and macroscopic forms of DM – like PBHs and PBH clusters

Dark Matter from Elementary Particles

By definition Dark Matter is non-luminous, while charged particles are the source of electromagnetic radiation. Therefore, neutral weakly interacting elementary particles are usually considered as Dark Matter candidates. If such neutral particles with mass m are stable, they freeze out in early Universe and form structure of inhomogeneities with the minimal characterstic scale

$$M = m_{Pl}\left(\frac{m_{Pl}}{m}\right)^2$$

- At m>> 1 GeV this scale corresponds to Cold Dark Matter (CDM) scenario
- Supersymmetric (SUSY) models naturally predict several candidates for such Weakly Interacting Massive Particles (WIMP)
- SUSY WIMP candidates were linked to a set of supesymmetric partners of the known particles to be discovered at the LHC.

“WIMP miracle”

- Freezing out of particles with mass of few hundred GeV and annihilation cross section of the order of weak interaction leads to their primordial abundance, which can explain dark matter.
- However direct search for such WIMPs doesn’t give positive result, as well as no SUSY particles are detected at the LHC
- It can imply a much wider list of DM candidates

The list of some physical candidates for DM

- Sterile neutrinos – physics of neutrino mass
- Axions – problem of CP violation in QCD
- Gravitinos – SUGRA and Starobinsky supergavity
- KK-particles: B_{KK1}
- Anomalous hadrons, O-helium ⟵ ***SIMP*** ***(strongly interacting massive particles)***
- Supermassive particles…
- Mirror and shadow particles,
- PBHs…

THE PUZZLES OF DIRECT DARK MATTER SEARCHES

See talk by R. Bernabei

DARK MATTER FROM CHARGED PARTICLES?

Baryonic Matter – atoms of stable quarks and charged lepton (electron)

- Ordinary matter consists of atoms
- Atoms consist of nuclei and electrons.
- Electrons are lightest charged particles – their stability is protected by the conservation of electric charge.
- Nuclei consist of nucleons, whose stability reflects baryon charge conservation.

In ordinary matter stable elementary particles are electrically charged, but bound in neutral atoms.

Dark Matter from Charged Particles?

By definition Dark Matter is non-luminous, while charged particles are the source of electromagnetic radiation. Therefore, neutral weakly interacting elementary particles are usually considered as Dark Matter candidates. If such neutral particles with mass m are stable, they freeze out in early Universe and form structure of inhomogeneities with the minimal characterstic scale

$$M = m_{Pl}\left(\frac{m_{Pl}}{m}\right)^2$$

- However, if charged particles are heavy, stable and bound within neutral « atomic » states they can play the role of composite Dark matter.
- Physical models, underlying such scenarios, their problems and nontrivial solutions as well as the possibilities for their test are the subject of the present talk.

« No go theorem » for -1 charge components

- ***If composite dark matter particles are « atoms », binding positive P and negative E charges, all the free primordial negative charges E bind with He-4, as soon as helium is created in SBBN.***
- ***Particles E with electric charge -1 form +1 ion [E He].***
- ***This ion is a form of anomalous hydrogen.***
- Its Coulomb barrier prevents effective binding of positively charged particles P with E. These positively charged particles, bound with electrons, become atoms of anomalous istotopes
- ***Positively charged ion is not formed, if negatively charged particles E have electric charge -2.***

Nuclear-interacting composite dark matter: O-helium « atoms »

If we have a stable double charged particle X^{--} *in excess over its partner* X^{++} *it may create Helium like neutral atom (O-helium) at temperature* $T < I_o$

Where:

$$I_o = Z_{He}^2 Z_\Delta^2 \alpha^2 m_{He} = 1.6 MeV$$

^{4}He is formed at T ~100 keV (t~100 s)
This means that it would rapidly create a neutral atom, in which all X^{--} are bound

$$X^{--} + {}^4He => (X\ He) + \gamma$$

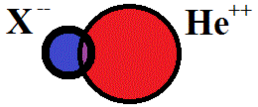

The Bohr orbit of O-helium « atom » is of the order of radius of helium nucleus.

$$R_o = 1/\left(ZZ_{He}\alpha m_{He}\right) = 2\cdot 10^{-13}\, cm$$

References

1. M.Yu. Khlopov, *JETP Lett.* 83 (2006) 1;
2. D. Fargion, M.Khlopov, C.Stephan, *Class. Quantum Grav.* 23 (2006) 7305;
2. M. Y. Khlopov and C. Kouvaris, *Phys. Rev.* D 77 (2008) 065002]

Constituents of composite dark matter

Few possible candidates for -2 charges:

Stable doubly charged "leptons" with mass >100 GeV (~1 TeV range):

- *AC « leptons » from almost commutative geometry*

D. Fargion, M.Khlopov, C.Stephan, Class. Quantum Grav. 23 (206) 7305

- *Technibaryons and technileptons from Walking Technicolor (WTC)*

M. Y. Khlopov and C. Kouvaris, Phys. Rev. D 77 (2008) 065002; M. Y. Khlopov and C. Kouvaris, Phys. Rev. D 78 (2008) 065040

Hadron-like bound states of:

- *Stable U-quark of 4-th family in Heterotic string phenomenology*

M.Yu. Khlopov, *JETP Lett.* 83 (2006) 1

- *Stable U-quarks of 5th family in the approach, unifying spins and charges*

N.S. Mankoc Borstnik, Mod. Phys. Lett. A 10 (1995) 587

M.Yu.Khlopov, A.G.Mayorov, E.Yu.Soldatov (2010), arXiv:1003.1144

WTC-model

*The ideas of Technicolor (TC) are revived with the use of SU(2) group for "walking" (not running) TC gauge constant *.*

1. *U and D techniquarks bound by Technicolor give mass to W and the Z bosons.*
2. *UU, UD, DD and their corresponding antiparticles are technibaryons and corresponding anti-technibaryons.*
3. *The electric charges of UU, UD, and DD are in general **y+1, y** and **y-1** respectively, where **y** is an arbitrary real number.*
4. *In order to cancel the **Witten global anomaly** the model requires in addition an existence of a fourth family of leptons.*
5. *Their electric charges are in terms of **y** respectively **(1 - 3y)/2** and **(-1 - 3y)/2.***
   *If **y=1**, both **stable doubly charged** technibaryons and technileptons are possible**.*

All these stable techniparticles will look like stable multiple charged leptons at LHC

References

*

F. Sannino and K. Tuominen, *Phys. Rev.* D 71 (2005) 051901 ;
D. K. Hong *et al*.,*Phys. Lett.* B 597 (2004) 89 ;
D. D. Dietrich *et al*., *Phys. Rev.* D 72 (2005) 055001 ;
S. B. Gudnason *et al*., *Phys. Rev.* D 73 (2006) 115003 ;
S. B. Gudnason *et al*, *Phys. Rev.* D 74 (2006) 095008]

**

M. Y. Khlopov and C. Kouvaris, Phys. Rev. D 77 (2008) 065002;

Techniparticle excess

- The advantage of WTC framework is that it provides definite relationship between baryon asymmetry and techniparticle excess.

$$\frac{TB}{B} = -\sigma_{UU}\left(\frac{L'}{B}\frac{1}{3\sigma_\zeta} + 1 + \frac{L}{3B}\right)$$

Here $\sigma_i \ (i = UU, \zeta)$ are statistical factors in equilibrium relationship between, TB, B, L and L'

The equilibrium is maintained by electroweak SU(2) sphalerons and similar relationship can hold true for any SU(2) dublets (like U quarks of 4th family or stable quarks of 5th family)

Relationship between TB and B

$$\xi = \frac{L'}{3B\sigma_\zeta} + 1 + \frac{L}{3B}$$

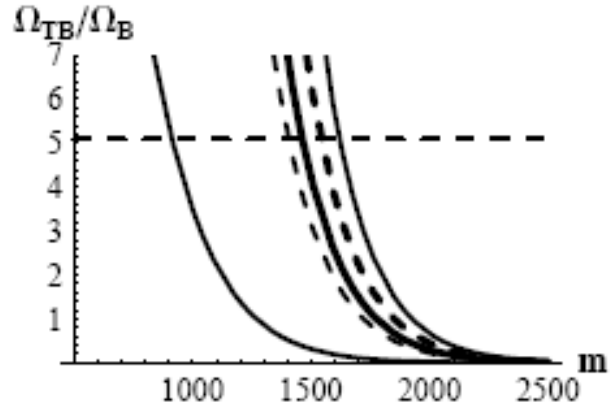

- L'=0, T*=150 GeV
  ξ =0.1; 1; 4/3; 2; 3

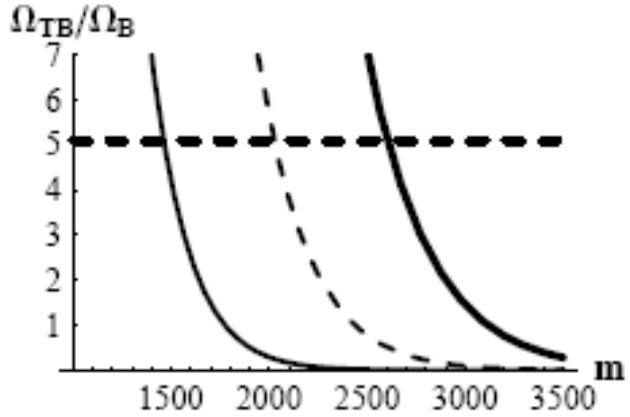

$\xi = 4/3$

- L'=0,

T*=150, 200, 250 GeV

Relationship between TB, L' and B

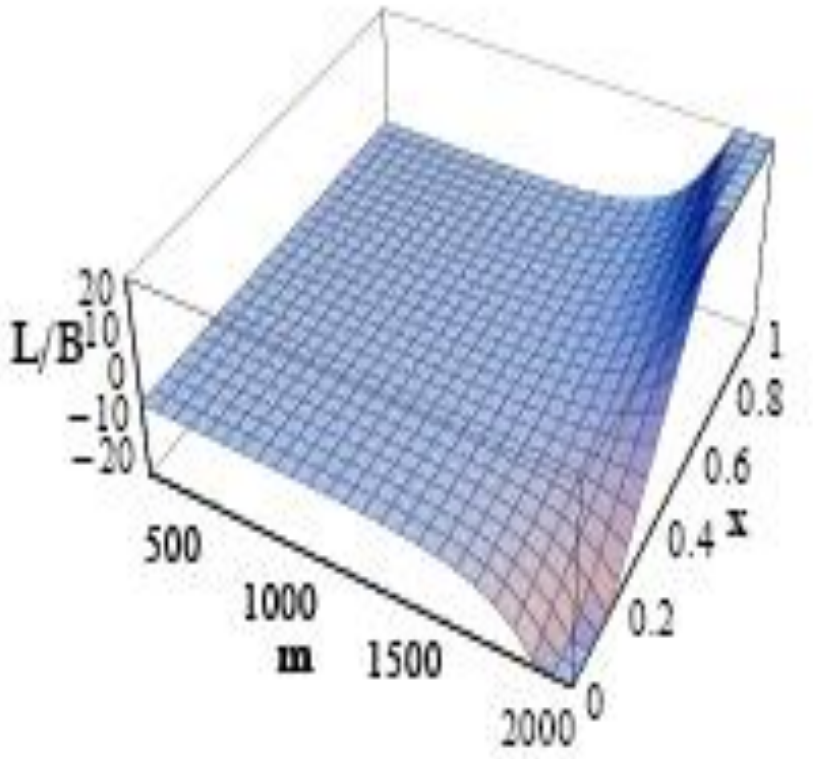

- x denotes the fraction of dark matter given by the technibaryon
- TB<0, L'>0 – two types of -2 charged techniparticles.

The case TB>0, L'>0 (TB<0, L'<0) gives an interesting possibility of (-2 +2) atom-like WIMPs, similar to AC model. For TB>L' (TB<L') no problem of free +2 charges

Stable multiple charged particles

WTC can lead to techniparticles with multiple charge

q	$UU(q+1)$	$UD(q)$	$DD(q-1)$	$\nu'(\frac{1-3q}{2})$	$\zeta(\frac{-1-3q}{2})$
1	**2**	1	0	-1	**-2**
3	**4**	3	**2**	**-4**	-5
5	**6**	5	**4**	-7	**-8**
7	**8**	7	**6**	**-10**	-11

-2n charged particles in WTC bound with n nuclei of primoridal He form Thomson atoms of XHe

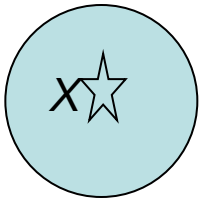

nHe

O-HELIUM DARK MATTER

O-helium dark matter

$$T < T_{od} = 1keV$$

$$n_b \langle \sigma v \rangle \left(m_p / m_o \right) t < 1$$

$$T_{RM} = 1eV$$

$$M_{od} = \frac{T_{RM}}{T_{od}} m_{Pl} \left(\frac{m_{Pl}}{T_{od}} \right)^2 = 10^9 M_{Sun}$$

- Energy and momentum transfer from baryons to O-helium is not effective and O-helium gas decouples from plasma and radiation
- O-helium dark matter starts to dominate
- On scales, smaller than this scale composite nature of O-helium results in suppression of density fluctuations, making O-helium gas Warmer than Cold Dark Matter

O-helium in Earth

- Elastic scattering dominates in the (OHe)-nucleus interaction. After they fall down terrestrial surface the in-falling OHe particles are effectively slowed down due to elastic collisions with the matter. Then they drift, sinking down towards the center of the Earth with velocity

$$V = \frac{g}{n\sigma v} \approx 80 S_3 A_{med}^{1/2} \, \mathrm{cm/s}.$$

Here $A_{med} \sim 30$ is the average atomic weight in terrestrial surface matter, $n = 2.4 \cdot 10^{24}/A_{med}$ is the number of terrestrial atomic nuclei, σv is the rate of nuclear collisions and $g = 980 \ \mathrm{cm/s^2}$.

O-helium experimental search?

- In underground detectors, (OHe) “atoms” are slowed down to thermal energies far below the threshold for direct dark matter detection. However, (OHe) nuclear reactions can result in observable effects.
- O-helium gives rise to less than 0.1 of expected background events in XQC experiment, thus avoiding severe constraints on Strongly Interacting Massive Particles (SIMPs), obtained from the results of this experiment.

It implies development of specific strategy for direct experimental search for O-helium.

O-HELIUM DARK MATTER IN UNDERGROUND DETECTORS

O-helium concentration in Earth

The O-helium abundance the Earth is determined by the equilibrium between the in-falling and down-drifting fluxes.

The in-falling O-helium flux from dark matter halo is

$$F = \frac{n_0}{8\pi} \cdot |\overline{V_h} + \overline{V_E}|,$$

where $\boldsymbol{V_h}$ is velocity of Solar System relative to DM halo (220 km/s), $\boldsymbol{V_E}$ is velocitv of orbital motion of Earth (29.5 km/s) and

$n_0 = 3 \cdot 10^{-4} S_3^{-1}\,\mathrm{cm}^{-3}$ is the local density of O-helium dark matter.

At a depth *L* below the Earth's surface, the drift timescale is ~*L/V.* It means that the change of the incoming flux, caused by the motion of the Earth along its orbit, should lead at the depth L ~ 10^5 cm to the corresponding change in the equilibrium underground concentration of OHe on the timescale

$$t_{dr} \approx 2.5 \cdot 10^2 S_3^{-1}\,\mathrm{s}$$

Annual modulation of O-helium concentration in Earth

The equilibrium concentration, which is established in the matter of underground detectors, is given by

$$n_{oE} = \frac{2\pi \cdot F}{V} = n_{oE}^{(1)} + n_{oE}^{(2)} \cdot sin(\omega(t - t_0)),$$

where $\omega = 2\pi/T$, T=1*yr* and t_o is the phase. The averaged concentration is given by

$$n_{oE}^{(1)} = \frac{n_o}{320 S_3 A_{med}^{1/2}} V_h$$

and the annual modulation of OHe concentration is characterized by

$$n_{oE}^{(2)} = \frac{n_o}{640 S_3 A_{med}^{1/2}} V_E$$

The rate of nuclear reactions of OHe with nuclei is proportional to the local concentration and the energy release in these reactions leads to ionization signal containing both constant part and annual modulation.

OHe solution for puzzles of direct DM search

- OHe equilibrium concentration in the matter of DAMA detector is maintained for less than an hour
- The process

$$OHe + (A,Z) \Rightarrow [OHe(A,Z)] + \gamma$$

is possible, in which only a few keV energy is released. Other inelastic processes are suppressed

- Annual modulations in inelastic processes, induced by OHe in matter. No signal of WIMP-like recoil
- Signal in DAMA detector is not accompanied by processes with large energy release. This signal corresponds to a formation of anomalous isotopes with binding energy of few keV

Potential of OHe-nucleus interaction

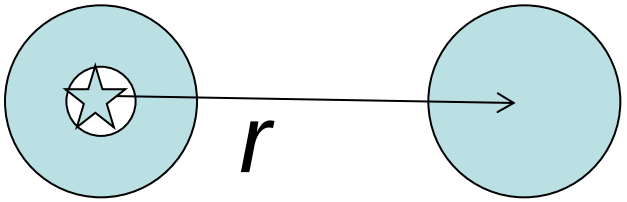

$$U_{Xnuc} = -2Z\alpha\left(1/r + 1/r_o\right)\exp\left(-2r/r_o\right)$$

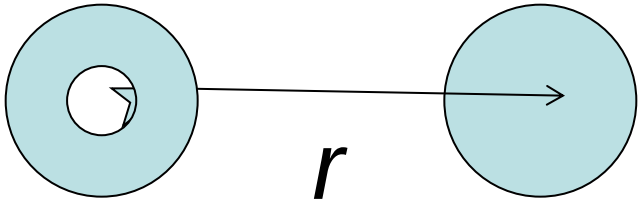

$$U_{Stark} = -\frac{2Z\alpha}{r^4}\frac{9}{2}r_o^3$$

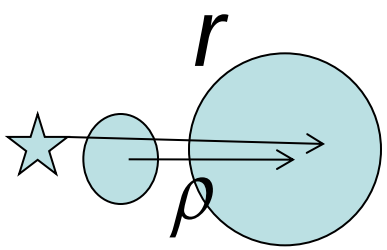

$$U_{Coul} = +\frac{2\alpha Z}{\rho} - \frac{2\alpha Z}{r}$$

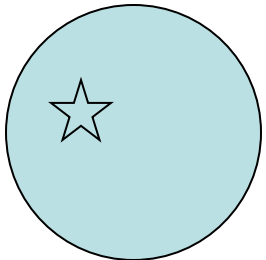

$$U_{osc} = -\left[\frac{(Z+2)\alpha}{R}\left(1-\left(\frac{r}{R}\right)^2\right)\right]$$

Formation of OHe-nucleus bound system

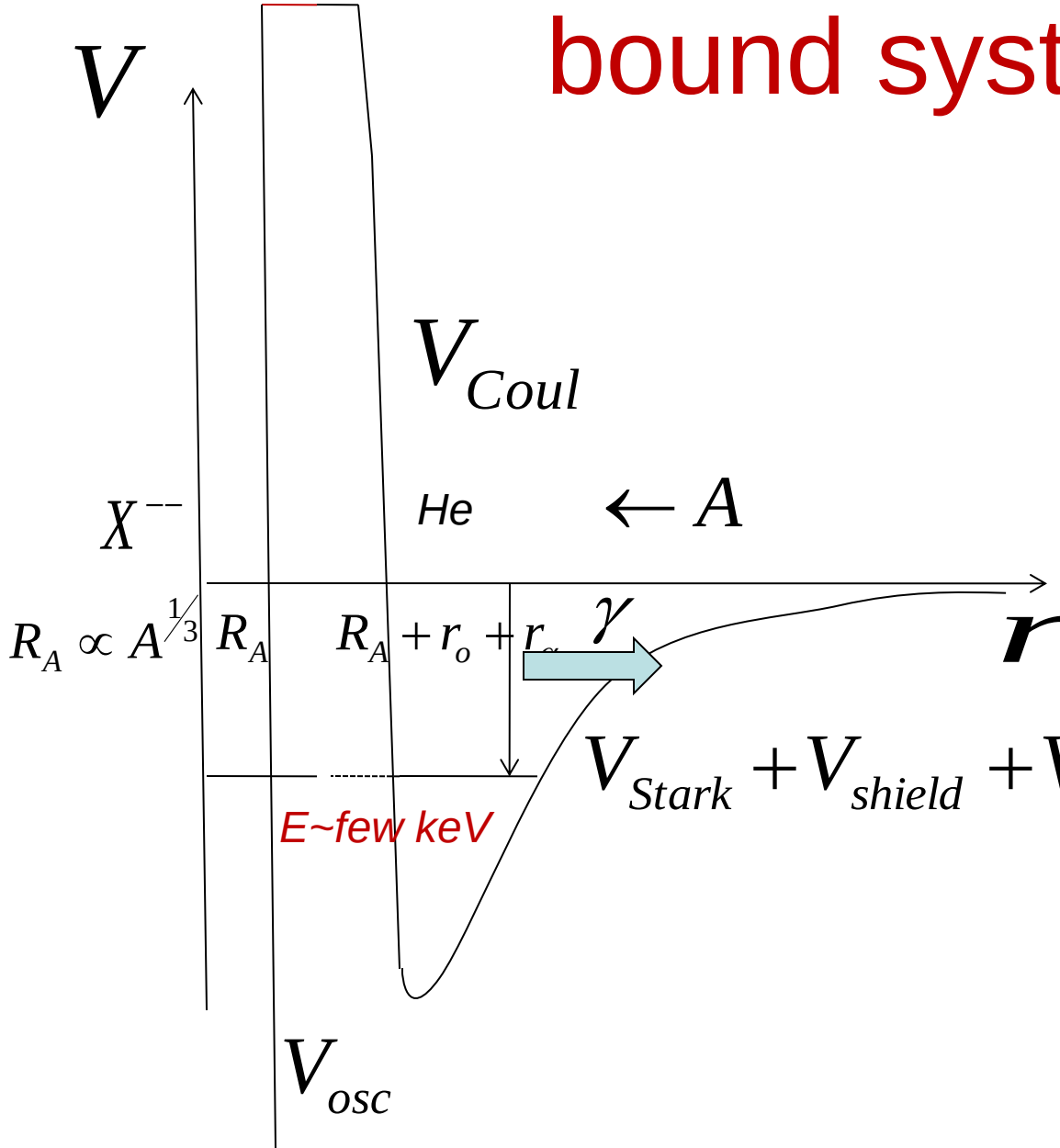

Due to shielded Coulomb potential of X, Stark effect and tail of nuclear Yukawa force OHe attracts the nucleus. Nuclear attarction causes OHe excitation and Coulomb repulsion is switched on. If the system emits a photon, OHe forms a bound state with nucleus but **beyond** *the nucleus with binding energy of few keV.*

Few keV Level in OHe-nucleus system

- The problem is reduced to a quantum mechanical problem of energy level of OHe-nucleus bound state in the potential well, formed by shielded Coulomb, Stark effect and Yukawa tail attraction and dipole-like Coulomb barrier for the nucleus in vicinity of OHe. The internal well is determined by oscillatory potential of X in compound (Z+2) nucleus, in which He is aggregated.
- The numerical solution for this problem is simplified for rectangular wells and walls, giving a few keV level for Na.

Rate of OHe-nucleus radiative capture

As soon as the energy of level is found one can use the analogy with radiative capture of neutron by proton with the account for:

- Absence of M1 transition for OHe-nucleus system (which is dominant for n+p reaction)
- Suppression of E1 transition by factor $f \sim 10^{-3}$, corresponding to isospin symmetry breaking

(in the case of OHe only isoscalar transition is possible, while E1 goes due to isovector transition only)

Reproduction of DAMA/NaI and DAMA/LIBRA events

The rate of OHe radiative capture by nucleus with charge Z and atomic number A to the energy level E in the medium with temperature T is given by

$$\sigma v = \frac{f\pi\alpha}{m_p^2}\frac{3}{\sqrt{2}}\left(\frac{Z}{A}\right)^2\frac{T}{\sqrt{Am_pE}}.$$

Formation of OHe-nucleus bound system leads to energy release of its binding energy, detected as ionization signal. In the context of our approach the existence of annual modulations of this signal in the range 2-6 keV and absence of such effect at energies above 6 keV means that binding energy of Na-Ohe system in DAMA experiment should not exceed 6 keV, being in the range 2-4 keV.

Annual modulation of signals in DAMA/NaI and DAMA/LIBRA events

The amplitude of annual modulation of ionization signal (measured in counts per day per kg, cpd/kg) is given by

$$\zeta = \frac{3\pi\alpha \cdot n_o N_A V_E t Q}{640\sqrt{2}A_{med}^{1/2}(A_I + A_{Na})} \frac{f}{S_3 m_p^2}\left(\frac{Z_i}{A_i}\right)^2 \frac{T}{\sqrt{A_i m_p E_i}} = 4.3 \cdot 10^{10} \frac{f}{S_3^2}\left(\frac{Z_i}{A_i}\right)^2 \frac{T}{\sqrt{A_i m_p E_i}}.$$

This value should be compared with the integrated over energy bins signals in DAMA/NaI and DAMA/LIBRA experiments and the results of these experiments can be reproduced for

$$E_{Na} = 3keV$$

DARK ATOM CONSTITUENTS AT ACCELERATORS

Complementarity in searches for Dark Matter

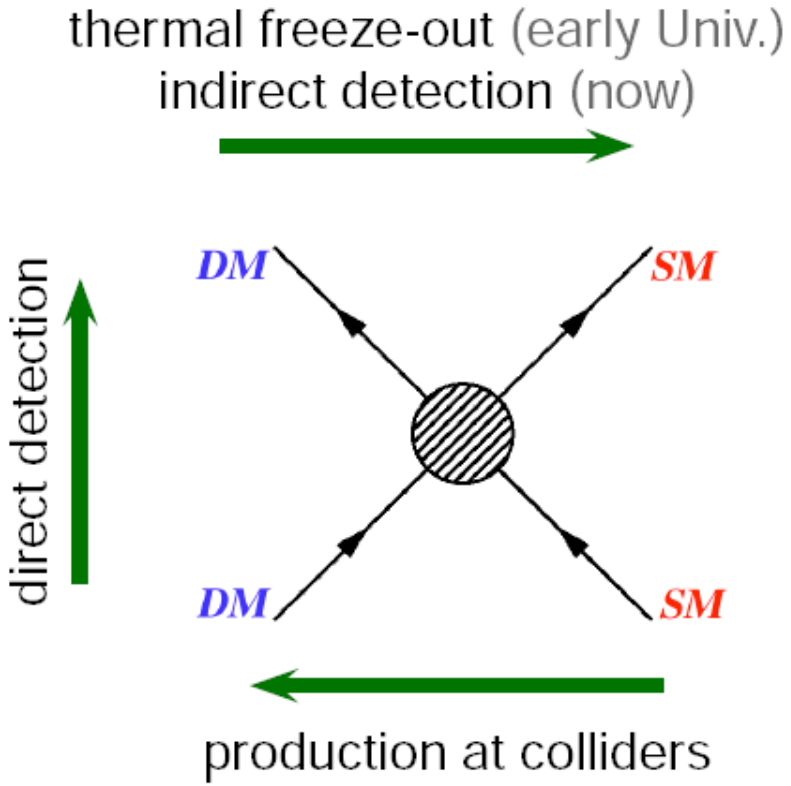

Usually, people use this illustration for complementarity in direct, indirect and accelerator searches for dark matter. However, we see that in the case of composite dark matter the situation is more nontrivial. We need charged particle searches to test dark atom model

Collider test for dark atoms

- Being the simplest dark atom model OHe scenario can not only explain the puzzles of direct dark matter searches, but also explain some possible observed indirect effects of dark matter. The latter explanation implies a very narrow range of masses of (meta-) stable double charged particles in vicinity of 1 TeV, what is the challenge for their search at the experiments at the LHC.

Search for multi-charge particles in the ATLAS experiment

Work is done in a frame of Multi-Charge Analysis Group

Search for Multi-charge Objects in pp collisions at $\sqrt{s} = 7$ TeV using the ATLAS detector

K.M. Belotsky[a], O. Bulekov[a], M. Jüngst[b], M.Yu.Khlopov[a,h], C. Marino[c], P. Mermod[d], H. Ogren[e], A. Romaniouk[a], Y. Smirnov[a], W. Taylor[f], B. Weinert[g], D. Zieminska[e], S. Zimmermann[g]

[a]*Moscow Engineering Physics Institute*
[b]*CERN*
[c]*University of Victoria*
[d]*Oxford University*
[e]*Indiana University*
[f]*York University*
[g]*University of Bonn*
[h]*University of Paris*

Our studies favor good chances for detection of multi-charge species in ATLAS detector

Searches for multiple charged particles in ATLAS experiment

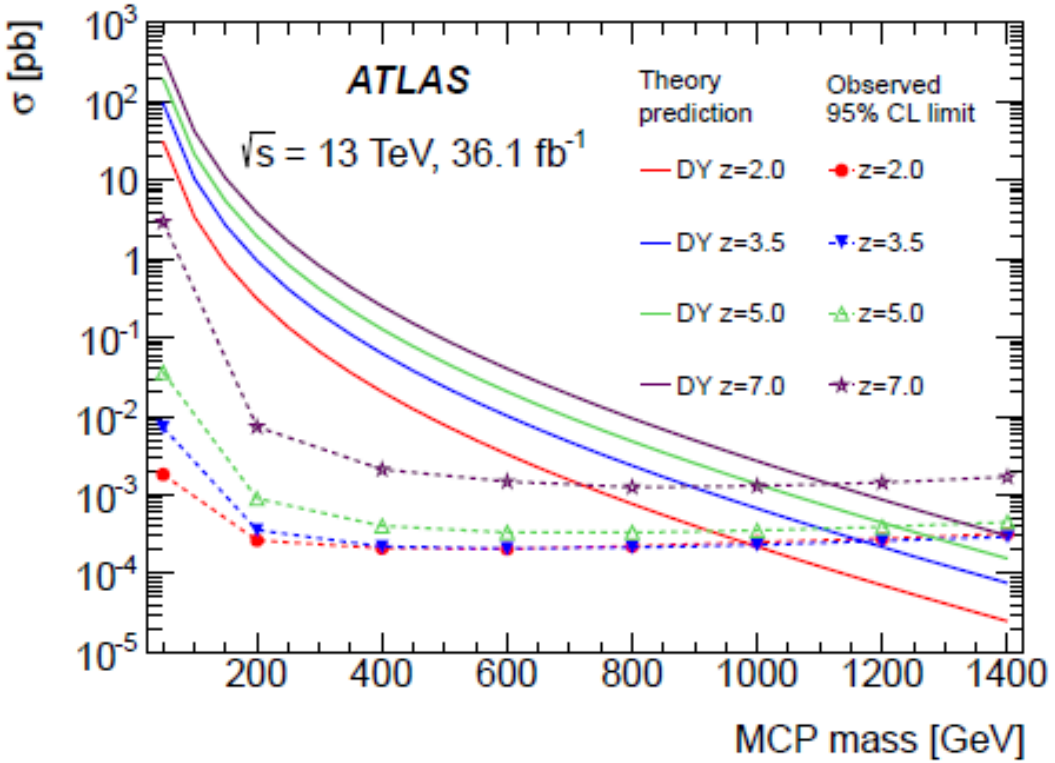

M>980 GeV for |q|=2e at 95% c.l.

[ATLAS Collaboration, Search for heavy long-lived multi-charged particles in proton-proton collisions at √ s= 13 TeV using the ATLAS detector. Phys. Rev. D 99, 052003 (2019)

The dark atom model can be probed due to upper limit on the mass of multiple charged constiuents (D.Sopin)

Experimentum crucis for composite dark matter at the LHC

Coming analysis of results of double charged particle searches at the LHC can cover all the range of masses, at which composite dark matter can explain excess of positron annihilation line in Galactic bulge,

$\|q\|/e$	z										
	2.0	2.5	3.0	3.5	4.0	4.5	5.0	5.5	6.0	6.5	7.0
Lower mass limit [TeV]	0.98	1.06	1.13	1.17	1.20	1.22	1.22	1.21	1.19	1.16	1.12

Remind that composite dark matter can explain excess of low energy positrons at M=1.25 TeV and high energy positrons at M<1 TeV. The latter is already excluded for double charged constituents.

[ATLAS Collaboration, Search for heavy long-lived multi-charged particles in proton-proton collisions at √ s= 13 TeV using the ATLAS detector. Phys. Rev. D 99, 052003 (2019)

STRONG PRIMORDIAL INHOMOGENEITY PROBES FOR INFLATION AND BARYOSYNTHESIS

Strong nonhomogeneities in nearly homogeneous and isotropic Universe

- **The standard approach is to consider homogeneous and isotropic world and to explain development of nonhomogeneous structures by gravitational instability, arising from small initial fluctuations.**

$$\delta \equiv \delta\rho / \rho << 1$$

- **However, if there is a tiny component, giving small contribution to total**

$\rho_i << \rho$ **its strong nonhomogeneity** $\delta_i \equiv (\delta\rho/\rho)_i > 1$

is compatible with small nonhomogeneity of the total density

$$\delta = (\delta\rho_i + \delta\rho)/\rho \approx (\delta\rho_i/\rho_i)(\rho_i/\rho) << 1$$

Such components naturally arise as consequences of particle theory, sheding new light on galaxy formation and reflecting in cosmic structures the fundamental structure of microworld.

Strong Primordial nonhomogeneities from the early Universe

- Cosmological **phase transitions** in inflationary Universe can give rise to unstable cosmological defects, retaining a replica in the form of primordial **nonlinear** structures (massive PBH clusters, archioles).
- Nonhomogenous baryosynthesis (including spontaneous baryosynthesis and leptogensis) in its extreme form can lead to **antimatter** domains in baryon asymmetrical inflationary Universe.

Strong nonhomogeneities of total density and baryon density are severely constrained by CMB data at large scales (and by the observed gamma ray background in the case of antimatter). However, their existence at smaller scales is possible.

Cosmological Phase transitions 1.

- At high temperature $T > T_{cr}$ spontaneously broken symmetry is restored, owing to thermal corrections to Higgs potential

$$V(\varphi, T=0) = -\frac{m^2}{2}\varphi^2 + \frac{\lambda}{4}\varphi^4 \Rightarrow V(\varphi, T) = \left(C\lambda T^2 - \frac{m^2}{2} \right)\varphi^2 + \frac{\lambda}{4}\varphi^4$$

- When temperature falls down below

$$T = T_{cr} \cong \langle \varphi \rangle = \frac{m}{\sqrt{\lambda}}$$

transition to phase with broken symmetry takes place.

Cosmological Phase transitions 2.

- Spontaneously broken symmetry can be restored on chaotic inflationary stage, owing to corrections in Higgs potential due to interaction of Higgs field with inflaton

$$V(\varphi,\psi=0)=-\frac{m^2}{2}\varphi^2+\frac{\lambda}{4}\varphi^4 \Rightarrow V(\varphi,\psi)=\left(\varepsilon\psi^2-\frac{m^2}{2}\right)\varphi^2+\frac{\lambda}{4}\varphi^4$$

- When inflaton field rolls down below

$$\psi=\psi_{cr}\cong\frac{m}{\sqrt{\varepsilon}}$$

transition to phase with broken symmetry takes place.

Topological defects

- In cosmological phase transition false (symmetric) vacuum goes to true vacuum with broken symmetry. Degeneracy of true vacuum states results in formation of topological defects.
- Discrete symmetry of true vacuum $\langle\varphi\rangle = \pm f$ leads to domains of true vacuum with $+f$ and $-f$ and false vacuum wall on the border.
- Continuous degeneracy $\langle\varphi\rangle = f\exp(i\theta)$ results in succession of singular points surrounded by closed paths with $\Delta\theta = 2\pi$. Geometrical place of these points is line – cosmic string.
- SU(2) degeneracy results in isolated singular points – in GUTs they have properties of magnetic monopoles.

U(1) model

$$V(\psi)=\frac{\lambda}{2}\left(\psi^2-f^2\right)^2$$

After spontaneous symmetry breaking infinitely degenerated vacuum

$$\psi = fe^{i\varphi/f}$$

experiences second phase transition due to the presence (or generation by instanton effects)

$$V(\varphi)=\Lambda^4\left(1-\cos\left(\varphi/f\right)\right)$$

to vacuum states

$$\theta\equiv\varphi/f=0,2\pi,\ldots$$

In particular, this succession of phase transitions takes place in axion models

Topological defects

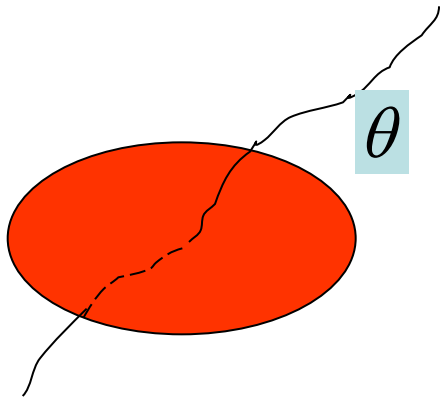

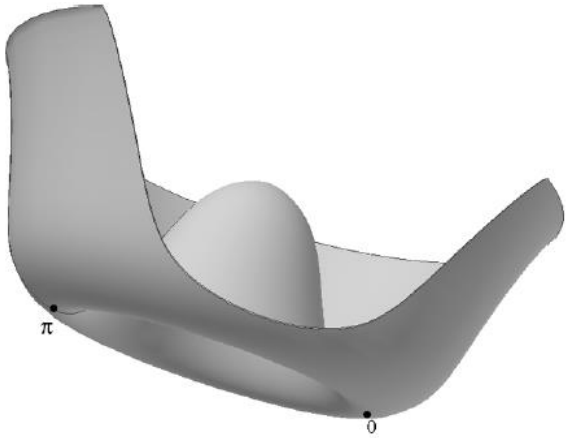

- Spontaneous breaking of U(1) symmetry results in the continuous degeneracy of vacua. In the early Universe the transition to phase with broken symmetry leads to formation of cosmic string network.
- The tilt in potential breaks continuous degeneracy of vacua. In the result string network converts into walls-bounded-by-strings structure in the second phase transition. This structure is unstable and decay, but the initial values of phase define the energy density of field oscillations.

Unstable topological defects

- This picture takes place in axion cosmology.
- The first phase transition gives rise to cosmic axion string network.
- This network converts in the second phase transition into walls-bounded-by-strings structure (walls are formed between strings along the surfaces $\alpha = \pi$), which is unstable.
- However, the energy density distribution of coherent oscillations of the field α follows the walls-bounded-by-strings structure.

Archioles structure

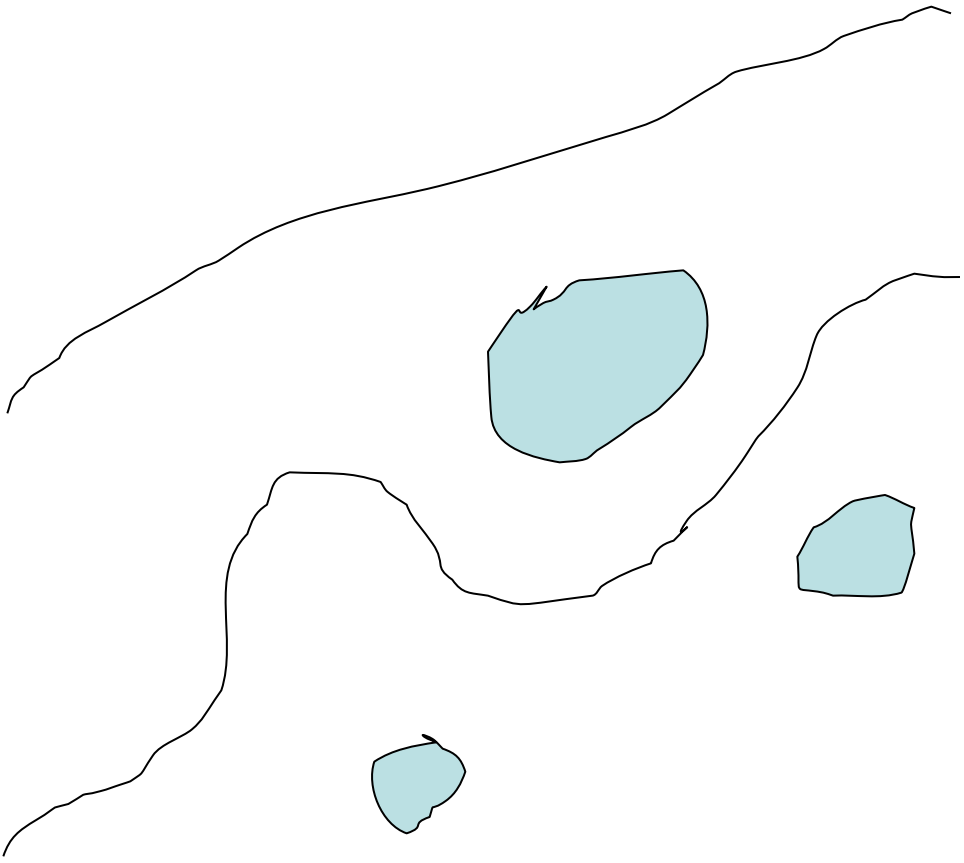

- **Numerical studies revealed that ~80% of string length corresponds to infinite Brownian lines, while the remaining ~20% of this length corresponds to closed loops with large size loops being strongly suppressed. It corresponds to the well known scale free distribution of cosmic strings.**
- **The fact that the energy density of coherent axion field oscillations reflects this property is much less known. It leads to a large scale correlation in this distribution, called archioles.**
- **Archioles offer possible seeds for large scale structure formation.**
- **However, the observed level of isotropy of CMB puts constraints on contribution of archioles to the total density and thus puts severe constraints on axions as dominant form of Dark Matter.**

Massive Primordial Black Holes

- Any object can form Black hole, if contracted within its gravitational radius. It naturally happens in the result of evolution of massive stars (and, possibly, star clusters).
- In the early Universe Black hole can be formed, if within cosmological horizon expansion can stop [Zeldovich, Novikov, 1966]. Since in the early Universe the total mass within horizon is small, it seems natural to expect that such Primordial Black holes should have very small mass (much smaller, than the mass of stars).
- However, cosmological consequences of particle theory can lead to mechanisms of intermediate and even supermassive BH formation.

Closed walls formation in Inflationary Universe

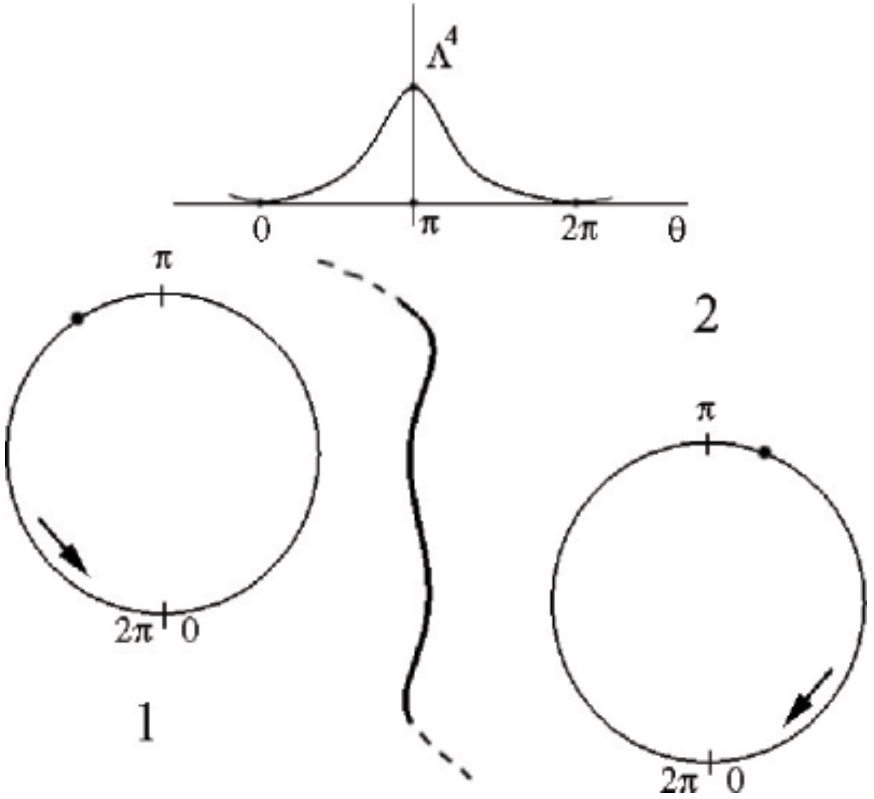

If the first U(1) phase transition takes place on inflationary stage, the value of phase θ , corresponding to e-folding N~60, fluctuates

$$\Delta\theta \approx H_{\text{infl}} / (2\pi f)$$

Such fluctuations can cross π

and after coherent oscillations begin,regions with $\theta > \pi$ occupying relatively small fraction of total volume are surrounded by massive walls

Massive PBH clusters

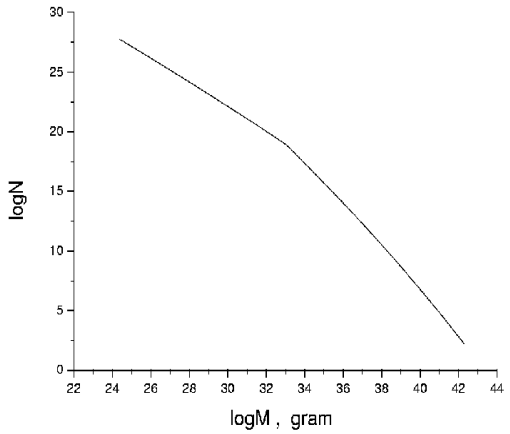

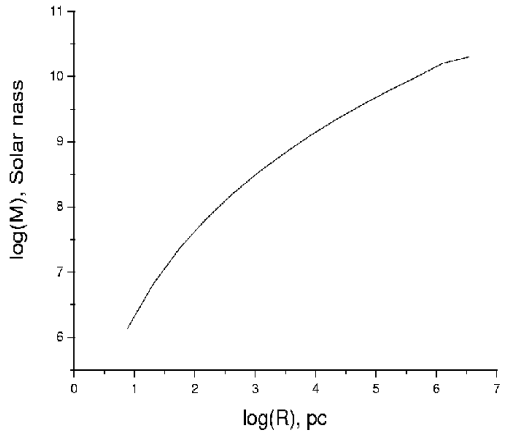

Each massive closed wall is accompanied by a set of smaller walls.

As soon as wall enters horizon, it contracts and collapses in BH.

Each locally most massive BH is accompanied by a cloud of less massive BHs.

The structure of such massive PBH clouds can play the role of seeds for galaxies and their large scale distribution.

Spectrum of Massive BHs

- The minimal mass of BHs is given by the condition that its gravitational radius exceeds the width of wall ($d \approx 2f/\Lambda^2$)

$$r_g = \frac{2M}{m_{Pl}^2} > d = \frac{2f}{\Lambda^2} \Rightarrow M_{\min} = f\left(\frac{m_{Pl}}{\Lambda}\right)^2$$

- The maximal mass is given by the condition that pieces of wall do not dominate within horizon, before the whole wall enters the horizon

$$R < \frac{3\sigma_w}{\rho_{tot}} \Rightarrow M_{\max} = f\left(\frac{m_{Pl}}{f}\right)^2\left(\frac{m_{Pl}}{\Lambda}\right)^2 \Rightarrow \frac{M_{\max}}{M_{\min}} = \left(\frac{m_{Pl}}{f}\right)^2$$

GW signals from closed wall collapse and BHs merging in clouds

- Closed wall collapse leads to primordial GW spectrum, peaked at $\nu_0 = 3 \cdot 10^{11} (\Lambda / f) Hz$ with energy density up to

$$\Omega_{GW} \approx 10^{-4} \left(f / m_{Pl} \right)$$

- At $f \sim 10^{14} GeV$ $\Omega_{GW} \sim 10^{-9}$
- For $1 < \Lambda < 10^{8} GeV$ $3 \cdot 10^{-3} Hz < \nu_0 < 3 \cdot 10^{5} Hz$

- Merging of BHs in BH cluster is probably detected by LIGO!.

Footprints of ALP

in PTA and JWST Observations

Shu-Yuan Guo (Yantai University)

Collaborate with

Maxim Khlopov, Xuewen Liu, Lei Wu,

Yongcheng Wu and Bin Zhu

arXiv:2306.17022

Generation of SGWB

Generation of SGWB

- Fractional energy density of gravitational waves:

Generation of SGWB

- Fractional energy density of gravitational waves:

$$\Omega_{\mathrm{gw}}(\ln f) = \frac{8\pi G}{3H_0^2} f\rho_{\mathrm{gw}}(t_0, f)$$

Generation of SGWB

- Fractional energy density of gravitational waves:

$$\Omega_{\mathrm{gw}}(\ln f) = \frac{8\pi G}{3H_0^2} f \rho_{\mathrm{gw}}(t_0, f)$$

$$\rho_{\mathrm{gw}}(t_0, f) = \int_{t_{\mathrm{sw}}}^{t_0} \frac{dt}{\left(1 + z(t)\right)^4} P_{\mathrm{gw}}(t, f') \frac{\partial f'}{\partial f}$$

(energy density in comoving volume)

Generation of SGWB

- Fractional energy density of gravitational waves:

$$\Omega_{\mathrm{gw}}(\ln f) = \frac{8\pi G}{3H_0^2} f \rho_{\mathrm{gw}}(t_0, f)$$

$$\rho_{\mathrm{gw}}(t_0, f) = \int_{t_{\mathrm{sw}}}^{t_0} \frac{dt}{\left(1 + z(t)\right)^4} P_{\mathrm{gw}}(t, f') \frac{\partial f'}{\partial f}$$

(energy density in comoving volume)

$$P_{\mathrm{gw}}(t, f') = \frac{dn(t, f')}{df'} P_{\mathrm{gw},i}$$

(GWs energy power)

Generation of SGWB

- For PBH

$$P_{\mathrm{gw},i}^{\mathrm{PBH}} \approx \frac{G}{C_2}\frac{\sigma^2}{f'^2}$$

Phys.Rev.D **104** (2021) 043005

Generation of SGWB

- For PBH

$$P_{\mathrm{gw},i}^{\mathrm{PBH}} \approx \frac{G}{C_2}\frac{\sigma^2}{f'^2}$$

Phys.Rev.D **104** (2021) 043005

$$\sigma = 4\Lambda^2 f_a$$

Generation of SGWB

- For PBH

$$P_{\mathrm{gw},i}^{\mathrm{PBH}} \approx \frac{G}{C_2}\frac{\sigma^2}{f'^2}$$

Phys.Rev.D **104** (2021) 043005

$$\sigma = 4\Lambda^2 f_a$$

leads to the fractional energy density as

$$\Omega_{\mathrm{gw}}^{\mathrm{PBH}}(\ln f) = \frac{32\sqrt{2}\pi}{21 C_2}\frac{\Omega_r^{1/4}}{H_0^{3/2}}\Gamma_s (G\sigma)^2 f^{-1/2}$$

Generation of SGWB

- For Wormhole

$$P_{\mathrm{gw},i}^{\mathrm{WH}} \approx \frac{\kappa^2}{4C_2 G}$$

Phys.Rev.D **104** (2021) 043005

Generation of SGWB

- For Wormhole

$$P_{\mathrm{gw},i}^{\mathrm{WH}} \approx \frac{\kappa^2}{4C_2 G}$$

Phys.Rev.D **104** (2021) 043005

κ—fraction of mass set in GWs

Generation of SGWB

- For Wormhole

$$P_{\mathrm{gw},i}^{\mathrm{WH}} \approx \frac{\kappa^2}{4C_2 G}$$

Phys.Rev.D **104** (2021) 043005

κ—fraction of mass set in GWs

leads to the fractional energy density as

$$\Omega_{\mathrm{gw}}^{\mathrm{WH}}(\ln f) = \frac{8\sqrt{2}\pi}{9C_2}\frac{\Omega_r^{1/4}}{H_0^{3/2}}\kappa^2\Gamma_s f^{3/2}$$

Generation of SGWB

- The generated SGWB:

$$\Omega_{\mathrm{GW}}(f) = \frac{8\pi\sqrt{2}\Omega_r^{1/4}}{3C_2H_0^{3/2}}\Gamma_s\left(\frac{1}{3}\kappa^2 f^{3/2} + \frac{4}{7}(G\sigma)^2 f^{-1/2}\right)$$

Generation of SGWB

- The generated SGWB:

$$\Omega_{\mathrm{GW}}(f) = \frac{8\pi\sqrt{2}\Omega_r^{1/4}}{3C_2H_0^{3/2}}\Gamma_s\left(\frac{1}{3}\kappa^2 f^{3/2} + \frac{4}{7}(G\sigma)^2 f^{-1/2}\right)$$

- PBH and WH exhibit distinct frequency dependencies, resulting in different dependencies on the size of the domain wall.

Generation of SGWB

- The generated SGWB:

$$\Omega_{\rm GW}(f) = \frac{8\pi\sqrt{2}\Omega_r^{1/4}}{3C_2H_0^{3/2}}\Gamma_s\left(\frac{1}{3}\kappa^2 f^{3/2} + \frac{4}{7}(G\sigma)^2 f^{-1/2}\right)$$

- PBH and WH exhibit distinct frequency dependencies, resulting in different dependencies on the size of the domain wall.

- The turning point of frequency corresponds to the location at where the ALP model can provide the largest size of PBH, i.e. $f_{\rm peak} = \sqrt{8 f_a \Lambda^2/(M_{\rm Pl}^2 t_0)}$.

Generation of SGWB

- The generated SGWB:

$$\Omega_{\rm GW}(f) = \frac{8\pi\sqrt{2}\Omega_r^{1/4}}{3C_2H_0^{3/2}}\Gamma_s\left(\frac{1}{3}\kappa^2 f^{3/2} + \frac{4}{7}(G\sigma)^2 f^{-1/2}\right)$$

- Casted in a power-law on experiments:

Generation of SGWB

- The generated SGWB:

$$\Omega_{\rm GW}(f) = \frac{8\pi\sqrt{2}\Omega_r^{1/4}}{3C_2H_0^{3/2}}\Gamma_s\left(\frac{1}{3}\kappa^2 f^{3/2} + \frac{4}{7}(G\sigma)^2 f^{-1/2}\right)$$

- Casted in a power-law on experiments:

$$\Omega_{\rm GW}(f) = \frac{2\pi^2}{3H_0^2} f^2 h_c(f)^2 = \frac{2\pi^2}{3H_0^2} A^2 f_{yr}^2 \left(\frac{f}{f_{\rm yr}}\right)^{5-\gamma}.$$

Generation of SGWB

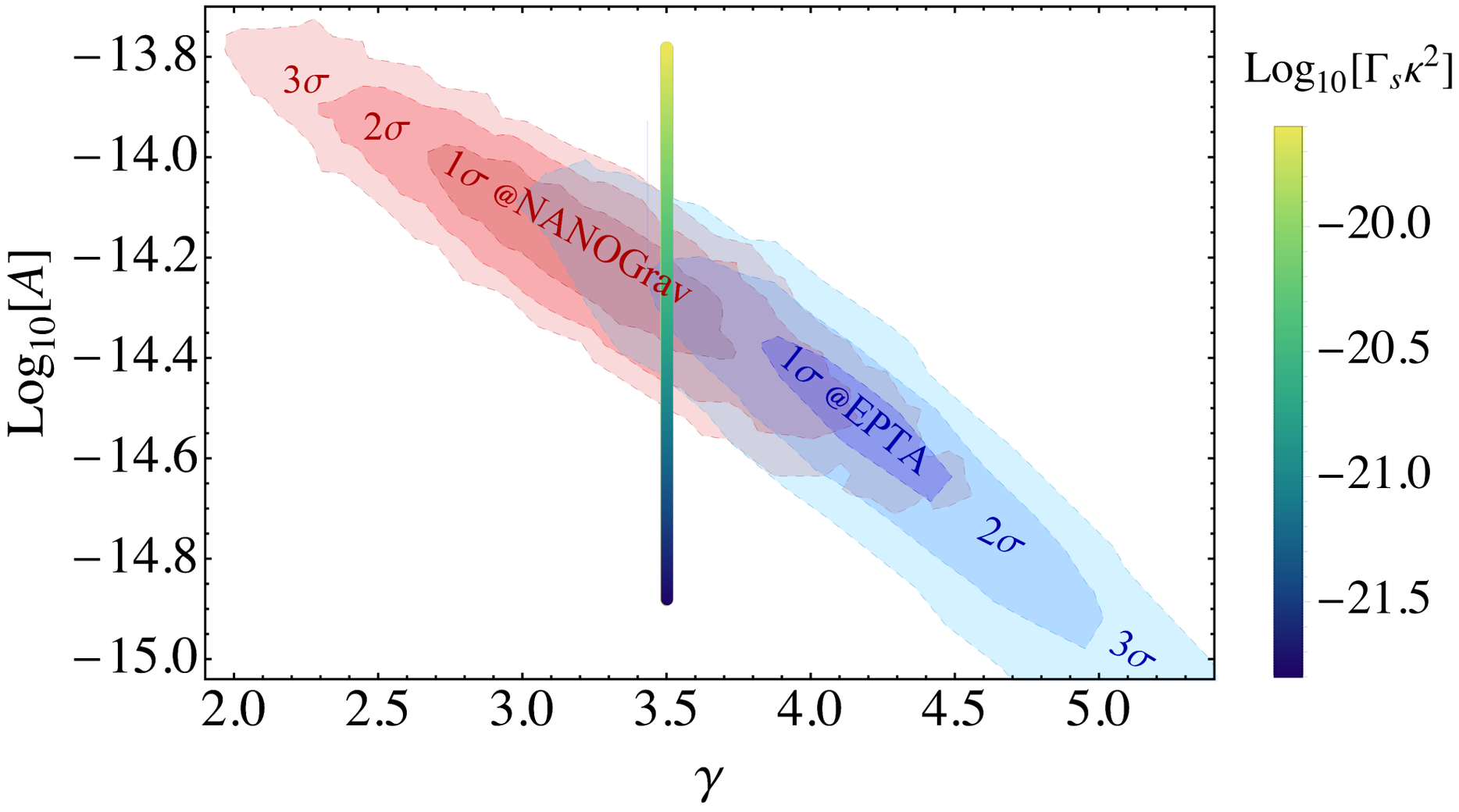

Generation of SGWB

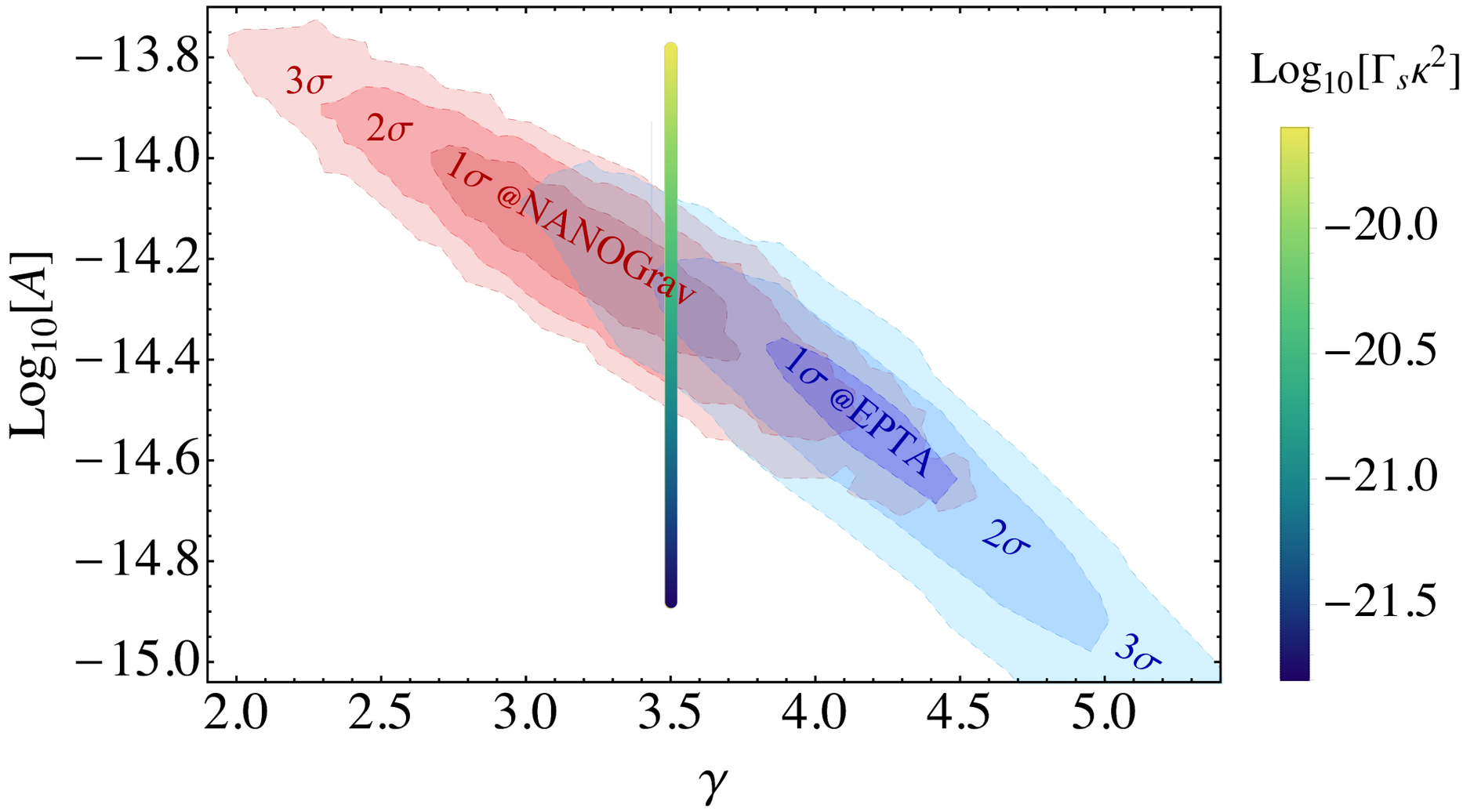

- NANOGrav shows consistent with EPTA in 2σ.

Generation of SGWB

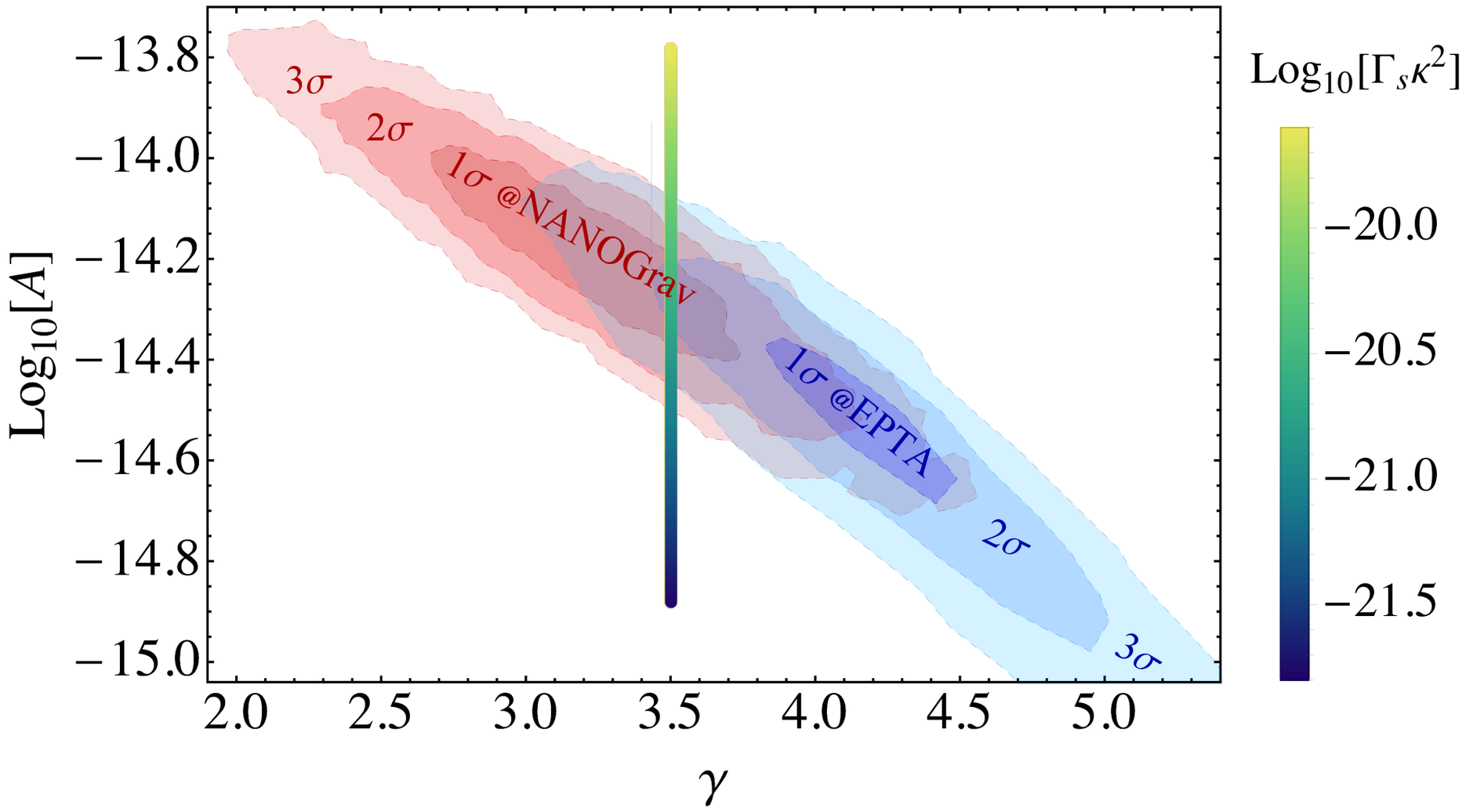

- NANOGrav shows consistent with EPTA in 2σ.
- Ω_{gw} from WH gives $\gamma = 3.5$, while Ω_{gw} from PBH gives $\gamma = 5.5$. Hence domain walls escape into baby universe give a better explanation on PTA data.

Generation of SGWB

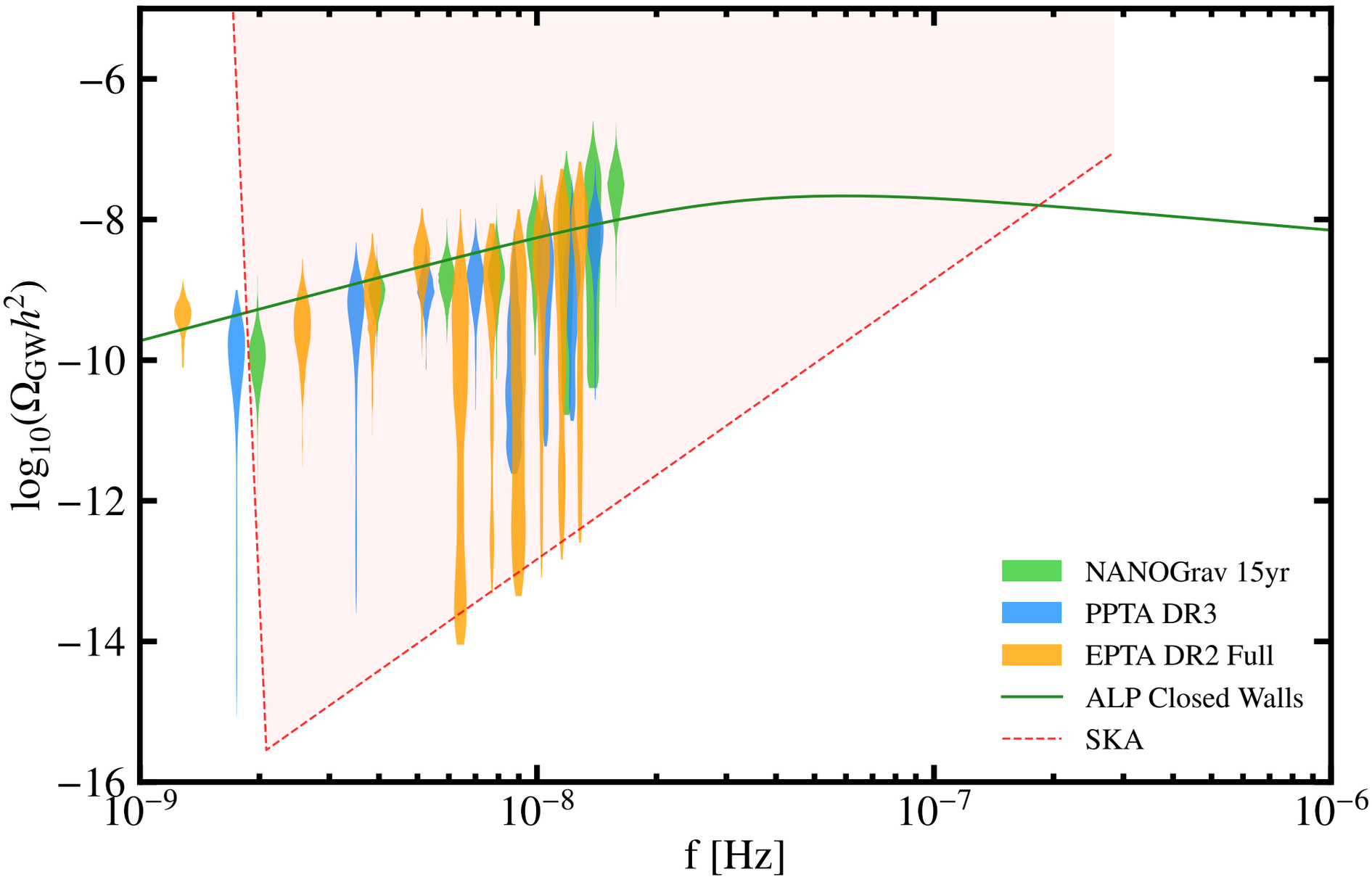

Generation of SGWB

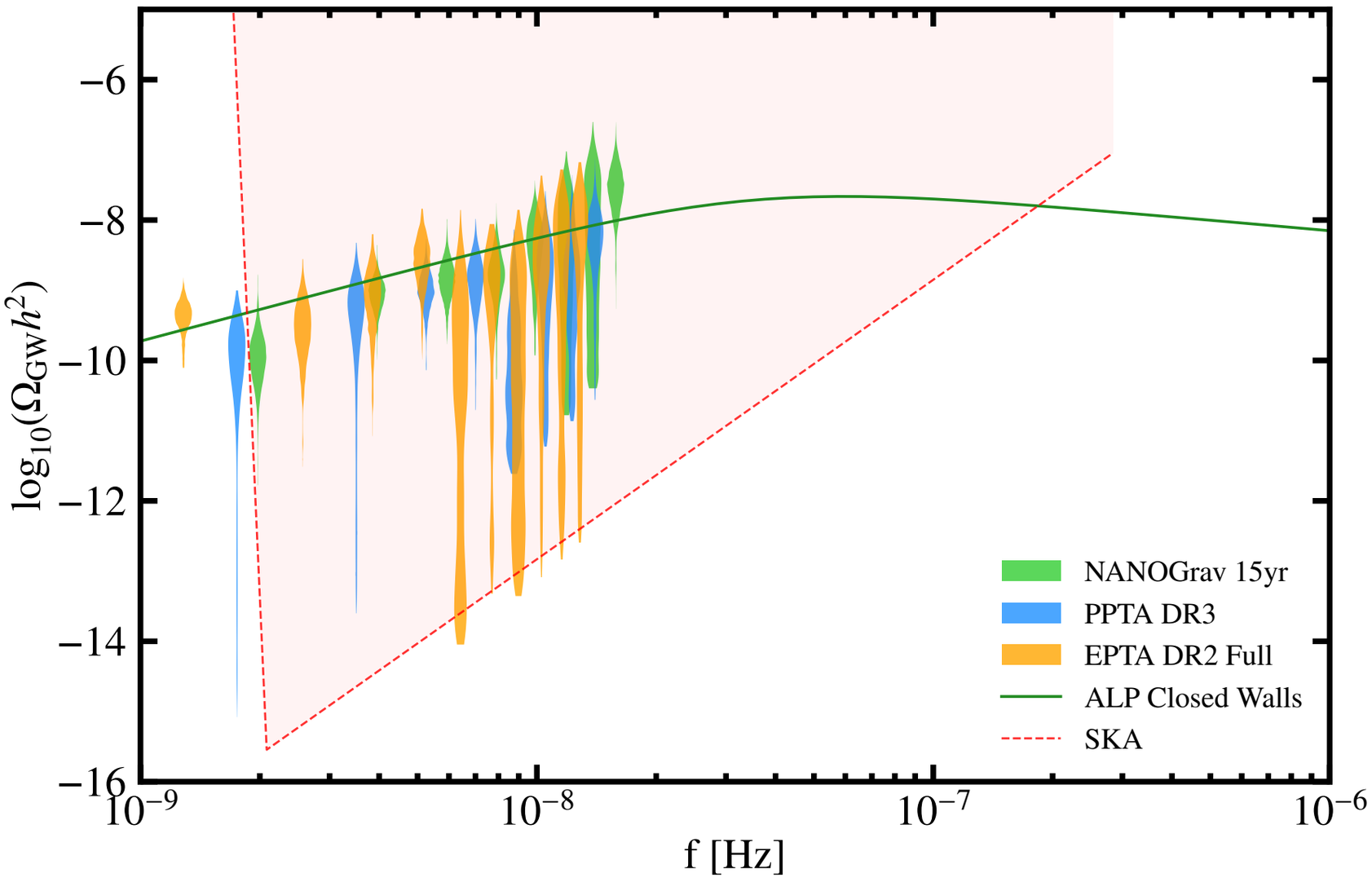

- Domain walls escape into baby universe show a compelling explanation for the PTA observations, with $f_{\rm peak} \geq f_{\rm yr}$.

Implication on JWST observations

Implication on JWST observations

- The James Webb Space Telescope reported six candidate massive galaxies with stellar mass greater than $10^{10} \odot$, at high redshift, $7.4 \leq z \leq 9.1$.

Implication on JWST observations

- The James Webb Space Telescope reported six candidate massive galaxies with stellar mass greater than $10^{10} \odot$, at high redshift, $7.4 \leq z \leq 9.1$.
- Challenges the current theoretical framework of early structure formation. Stellar mass of a galaxy is constrained by the mass function of dark matter halos.

Implication on JWST observations

- The James Webb Space Telescope reported six candidate massive galaxies with stellar mass greater than $10^{10} \odot$, at high redshift, $7.4 \leq z \leq 9.1$.
- Challenges the current theoretical framework of early structure formation. Stellar mass of a galaxy is constrained by the mass function of dark matter halos.
- Seeds effect of the ALP may modify the power spectrum at small scale, results in cumulative massive stellar mass.

Implication on JWST observations

- Comoving mass density above the threshold, in dark matter halos:

Implication on JWST observations

- Comoving mass density above the threshold, in dark matter halos:

$$\rho(M_\star \geq M_\star^{\rm obs}) = f_b\ \epsilon_\star \int_{M_h^{\rm cut}}^{\infty} M_h \frac{dn(z_{\rm obs}, M_h)}{dM_h} dM_h$$

Implication on JWST observations

- Comoving mass density above the threshold, in dark matter halos:

$$\rho(M_\star \geq M_\star^{\rm obs}) = f_b\ \epsilon_\star \int_{M_h^{\rm cut}}^{\infty} M_h \frac{dn(z_{\rm obs}, M_h)}{dM_h} dM_h$$

M_h—halo mass

$M_\star$—stellar mass

Implication on JWST observations

- Comoving mass density above the threshold, in dark matter halos:

$$\rho(M_\star \geq M_\star^{\rm obs}) = f_b\ \epsilon_\star \int_{M_h^{\rm cut}}^{\infty} M_h \frac{dn(z_{\rm obs}, M_h)}{dM_h} dM_h$$

M_h—halo mass

$M_\star$—stellar mass

f_b—baryon fraction

$\epsilon_\star$—star formation efficiency

Implication on JWST observations

- Comoving mass density above the threshold, in dark matter halos:

$$\rho(M_\star \geq M_\star^{\rm obs}) = f_b\ \epsilon_\star \int_{M_h^{\rm cut}}^{\infty} M_h \frac{dn(z_{\rm obs}, M_h)}{dM_h} dM_h$$

M_h—halo mass

$M_\star$—stellar mass

f_b—baryon fraction

$\epsilon_\star$—star formation efficiency

$M_\star = f_b \epsilon_\star M_h$

Implication on JWST observations

- Distribution of the ALP domain walls:

Implication on JWST observations

- Distribution of the ALP domain walls:

$$\frac{dn}{dM} = \frac{\Gamma_s}{2}\frac{1}{t_{\rm eq}^{3/2}}(4\pi\sigma)^{3/4}M^{-7/4}$$

Implication on JWST observations

- Distribution of the ALP domain walls:

$$\frac{dn}{dM} = \frac{\Gamma_s}{2}\frac{1}{t_{\rm eq}^{3/2}}(4\pi\sigma)^{3/4}M^{-7/4}$$

Γ_s—domain wall contour formation rate

Implication on JWST observations

- Distribution of the ALP domain walls:

$$\frac{dn}{dM} = \frac{\Gamma_s}{2} \frac{1}{t_{\rm eq}^{3/2}} (4\pi\sigma)^{3/4} M^{-7/4}$$

Γ_s—domain wall contour formation rate

$t_{\rm eq}$—time of matter-radiation equality

Implication on JWST observations

- Distribution of the ALP domain walls:

$$\frac{dn}{dM} = \frac{\Gamma_s}{2}\frac{1}{t_{\rm eq}^{3/2}}(4\pi\sigma)^{3/4}M^{-7/4}$$

Γ_s—domain wall contour formation rate

$t_{\rm eq}$—time of matter-radiation equality

$\sigma(\Lambda, f_a)$—domain wall tension

Joint constraints from JWST and ALP searching

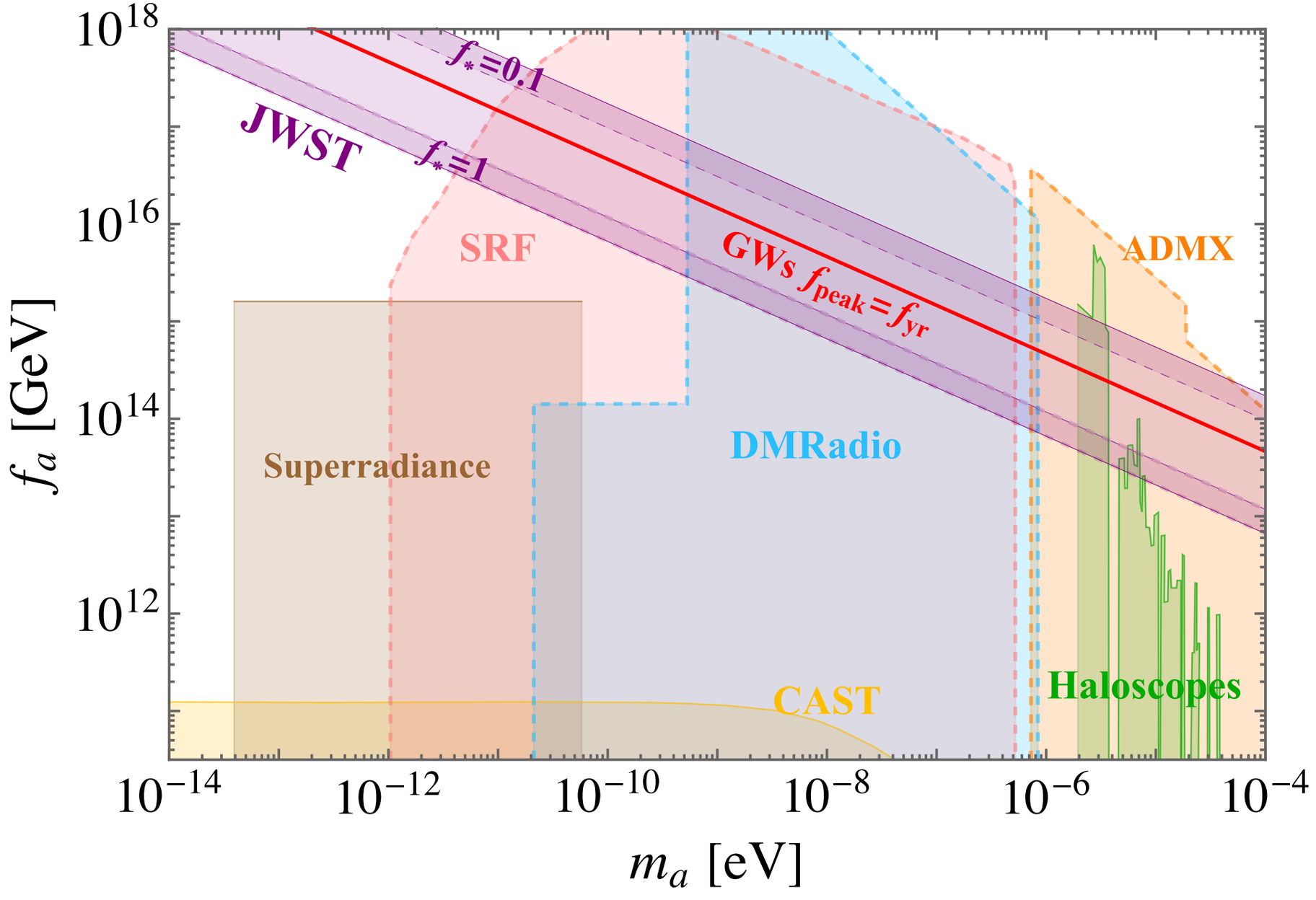

Joint constraints from JWST and ALP searching

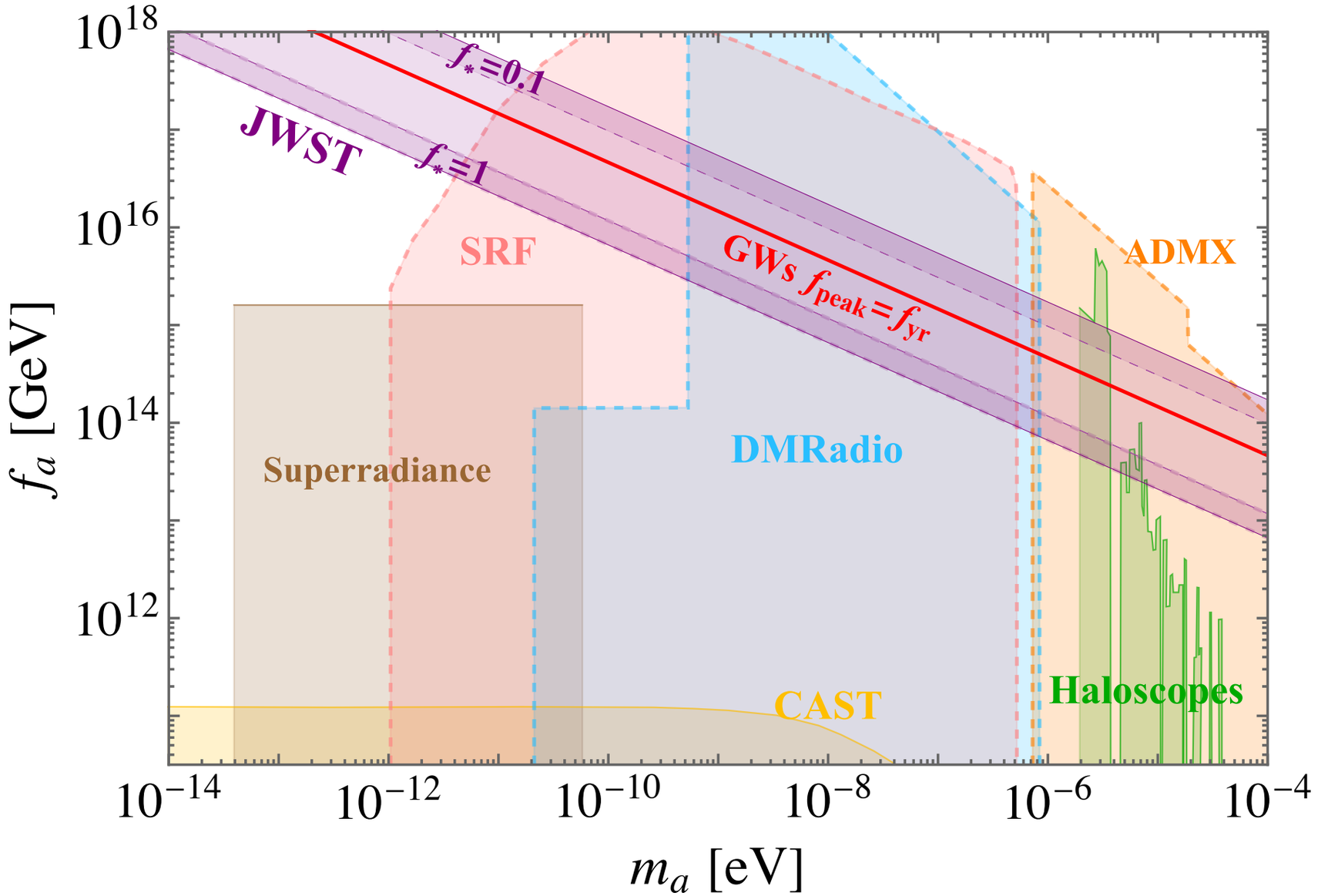

- The (f_a, m_a), which provide suitable GWs peak frequency, lie in the allowed parameter region to give out the JWST observations. And could be probed by the future axion experiments.

Conclusion

- We explore the characteristics of the SGWB within a typical ALP model. We discover that the domain walls, resulting from ALPs fluctuations during inflation, which escape into baby universes and radiate energy by GW, can effectively account for the recent nano-Hertz SGWB observations.
- Additionally, the initial fluctuations of ALPs play a crucial role in the formation of cosmological structures, giving rise to the massive galaxies observed by JWST. Our findings demonstrate that the ALP parameters capable of explaining PTA data also align with the observations made by JWST. Consequently, we establish a concise framework that encompasses both of these observations.

ANTIMATTER STARS IN BARYON ASYMMETRIC UNIVERSE

Antimatter from nonhomogeneous baryosynthesis

- Baryon excess B>0 can be generated nonhomogeneously B(x).
- Any nonhomogeneous mechanism of BARYON excess generation B(x) leads in extreme form to ANTIBARYON excess in some regions.

Survival of antimatter domains

Diffusion of baryons and antibaryons to the border of domain results in eating of antimatter by surrounding baryonic matter.

$$\partial n_b/\partial t = D(t)\partial^2 n_b/\partial x^2 - \alpha n_b \qquad \text{where} \qquad D(t) \approx \frac{3T_\gamma c}{2\rho_\gamma \sigma_T}$$

The minimal surviving scale is given by

$$d \approx \frac{c}{\sqrt{\frac{8\pi}{3}G\rho_0}} \frac{T_p}{m} \sqrt{\frac{m}{T_{rec}}} \int_{T_p/T_{rec}}^{1} \frac{dy}{y^{3/2}} = \frac{2c}{\sqrt{\frac{8\pi}{3}G\rho_0}} \sqrt{\frac{T_p}{m}}$$

which is about $d \sim 3/h$ kpc.

Nonhomogeneous spontaneous baryosynthesis

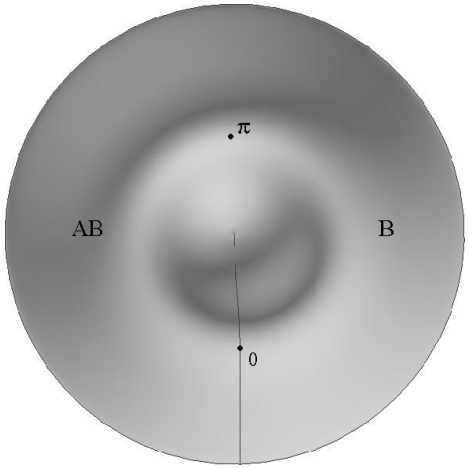

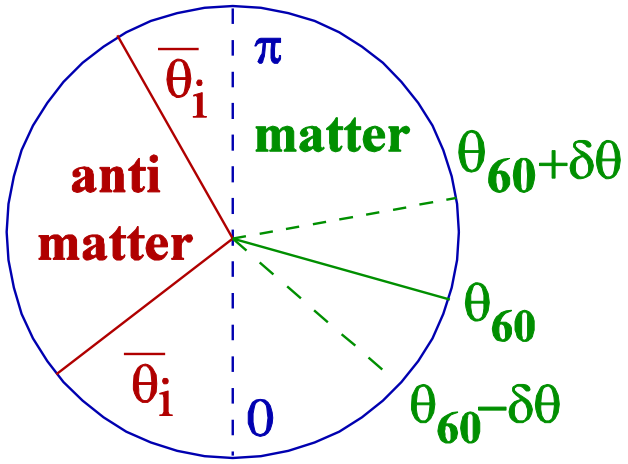

- Model of spontaneous baryosynthesis provides quantitative description of combined effects of inflation and nonhomogeneous baryosynthesis, leading to formation of antimatter domains, surviving to the present time.

Antimatter in galaxies

Number of e-fold	Number of domains	Size of domain
59	0	$1103 Mpc$
55	$5.005 \cdot 10^{-14}$	$37.7 Mpc$
54	$7.91 \cdot 10^{-10}$	$13.9 Mpc$
52	$1.291 \cdot 10^{-3}$	$1.9 Mpc$
51	0.499	$630 kpc$
50	74.099	$255 kpc$
49	$8.966 \cdot 10^{3}$	$94 kpc$
48	$8.012 \cdot 10^{5}$	$35 kpc$
47	$5.672 \cdot 10^{7}$	$12 kpc$
46	$3.345 \cdot 10^{9}$	$4.7 kpc$
45	$1.705 \cdot 10^{11}$	$1.7 kpc$

Numerical simulations show that within the modern horizon possible amount of antimatter domains, with the size exceeding the survival scale and thus surviving to the present time, can be comparable with the total number of galaxies.

In our Galaxy from 1000 to 100000 antimatter stars can exist in a form of antimatter globular cluster (Khlopov, 1998). Being in halo, such cluster is a faint gamma ray source, but antimatter from it pollutes Galaxy and can be observed indirectly by annihilation, or directly as anti-meteorites or antinuclei in cosmic rays.

Antimatter pollution of Galaxy

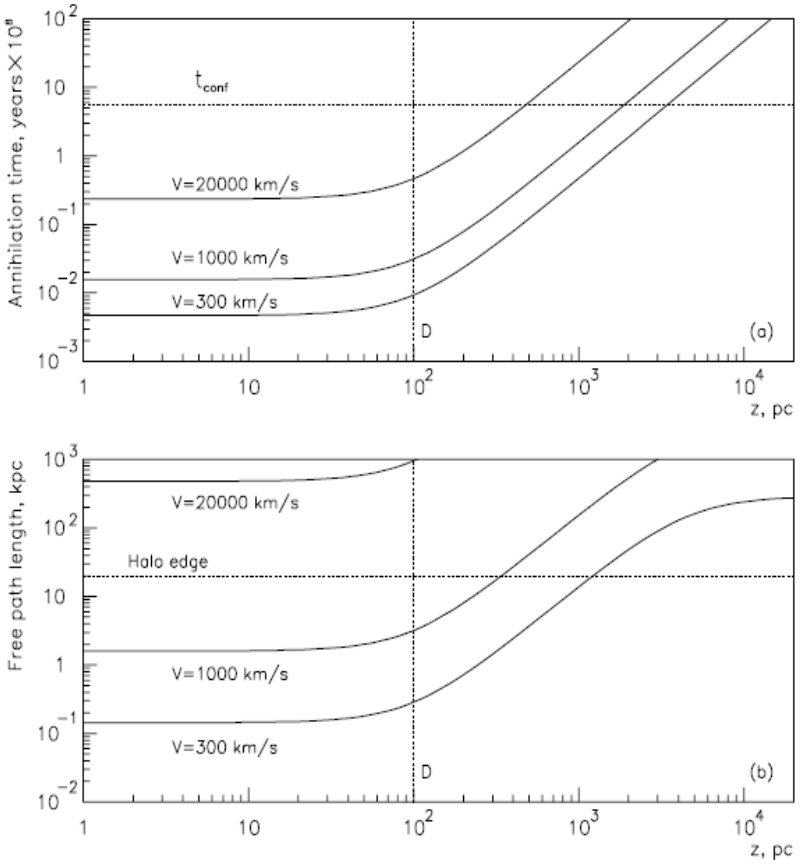

- Since antihydrogen is dominant in antimatter composition, the Galaxy is dominantly polluted by antiprotons.
- Their lifetime in Galaxy depends on their velocity and density of surrounding matter.

Gamma background from antimatter annihilation in Galaxy

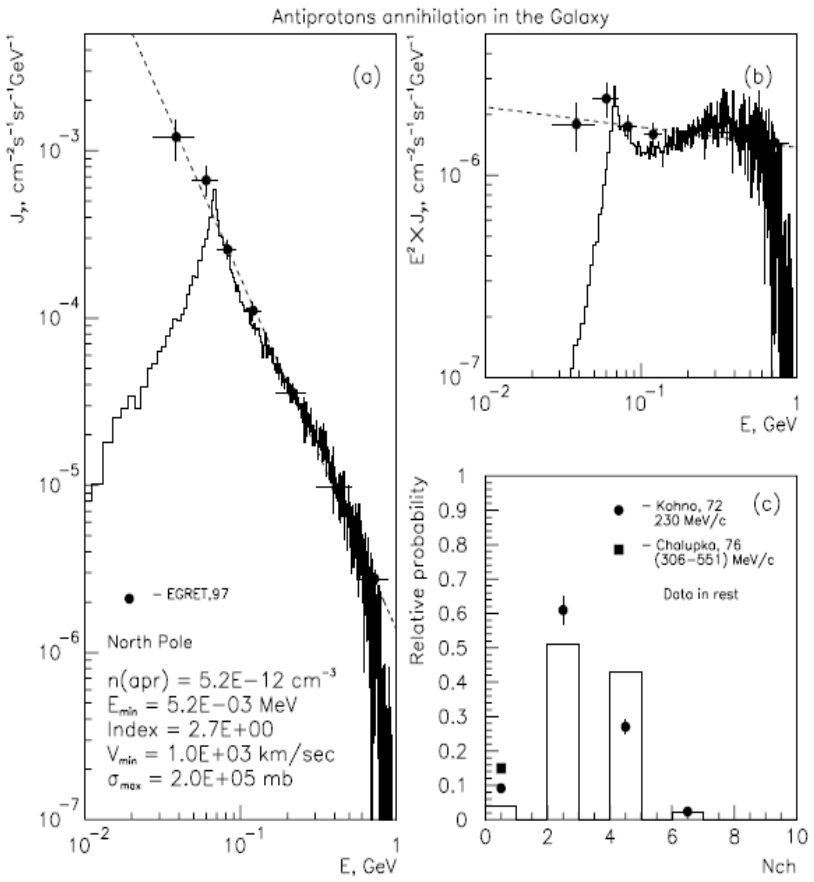

- Antiproton annihilation can reproduce gamma background observed by EGRET in the range tens-hundreds MeV.
- It can not be considered as PROOF for existence of antimatter stars – only pieces of antimatter (antihelium nuclei, antimeteorites) can provide such PROOF.

Cosmic antihelium test for antimatter stars in Galaxy

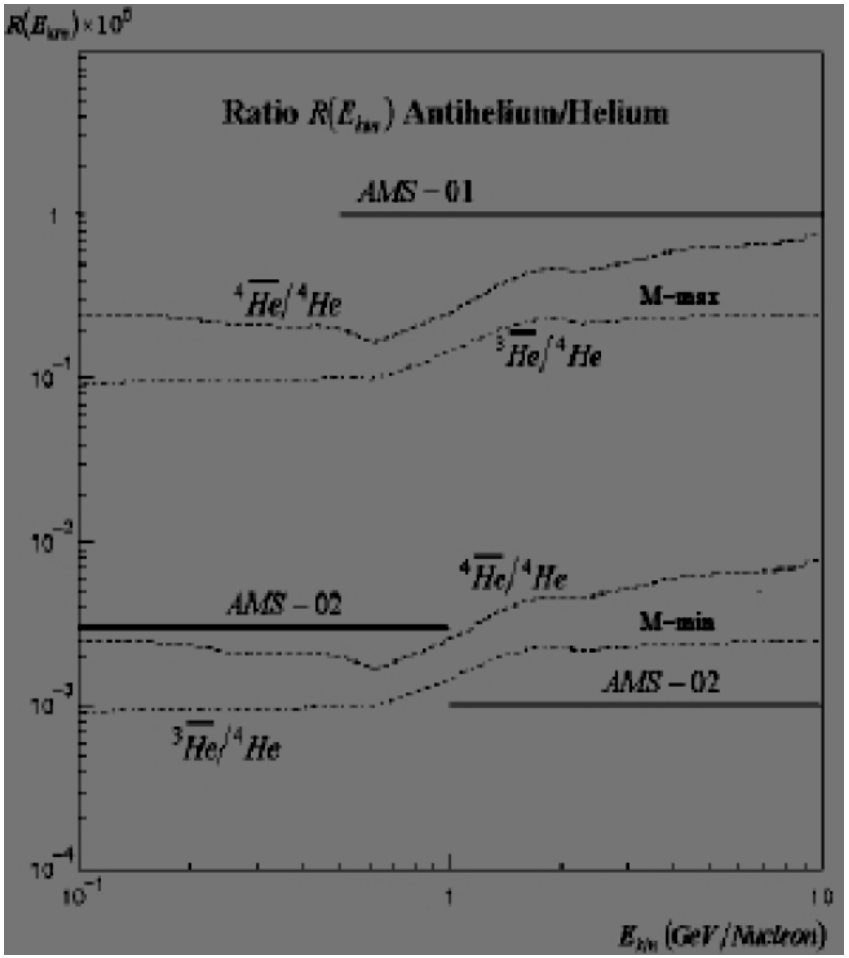

- **Nonhomogeneous baryosynthesis in extreme form leads to antimatter domains in baryon asymmetrical Universe**
- **To survive in the surrounding matter domain should be sufficiently large, and to have sufficiently high internal antibaryon density to form stars. It gives minimal estimation of possible amount of antimatter stars in Galaxy**
- **The upper limit comes from observed gamma background**
- **Assuming that antihelium component of cosmic rays is proportional to the fraction of antimatter stars in the total mass of Galaxy, it is possible to test this hypothesis initially in PAMELA and then completely in AMS-02 experiment**

Antihelium-4 candidates!

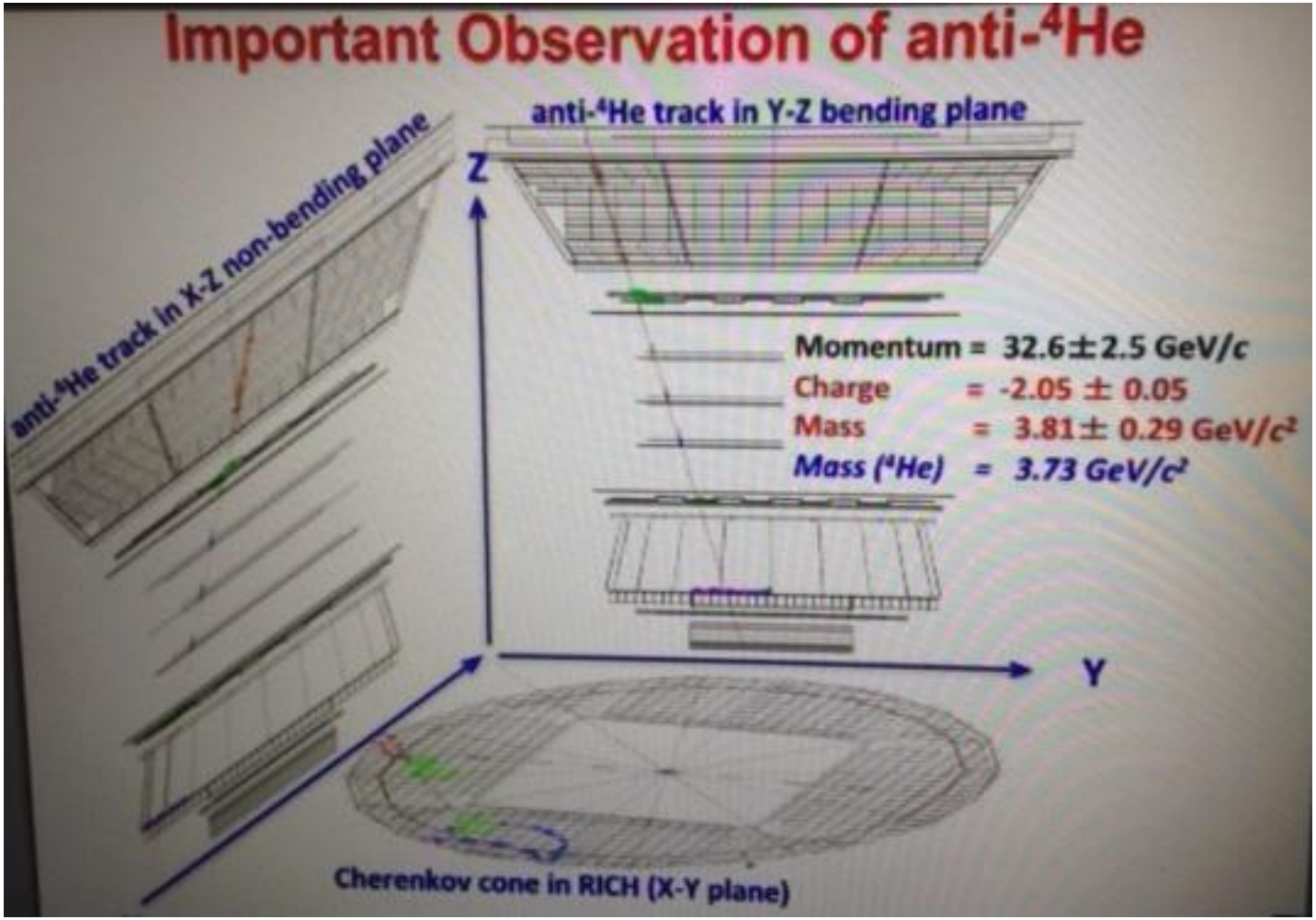

Probability 1/300 of background origin - Samuel Ting 24 May 2018
No possible background interpretation - Samuel Ting 8 June 2023

Future confirmation of cosmic antiHe-4?

AMS02 has an unprecedented sensitivity to antinuclear component of cosmic rays.
It puts on the collaboration high responsibility for quality its published results.
The experiment is continued until 2028 to increse the statistics, reject all the possible backgrounds and publish highly reliable data on the existence of antiHe-4 component of cosmic rays, sheding light on the form of antimatter celestial objects in our Galaxy.

Conclusions

Modern Standard cosmology is based on BSM physics and there should be no surprize that BSM features start to appear in the data of DM direct searches, PTA, JWST and AMS02.

We are coming to the era of great cosmological discoveries, which I hope will be subject of our future Bled Workshops.